Microreactor for Remote Canadian Communities

by

Jordan Crowell

A Thesis submitted to the
School of Graduate and Postdoctoral Studies in partial
fulfillment of the requirements for the degree of

Master of Applied Science in Nuclear Engineering

Department of Energy and Nuclear Engineering
Faculty of Engineering and Applied Science
University of Ontario Institute of Technology (Ontario Tech University)
Oshawa, Ontario, Canada
November 2022

Thesis Examination Information

Submitted by: **Jordan Crowell**

Master of Applied Science in Nuclear Engineering

Thesis title: Microreactor for Remote Canadian Communities

An oral defence of this thesis took place on November 7, 2022, in front of the following examining committee:

Examining Committee:

Chair of Examining Committee	Dr. Jennifer McKellar
Research Supervisor	Dr. Eleodor Nichita
Examining Committee Member	Dr. Kirk Atkinson
Thesis Examiner	Dr. Glenn Harvel

The above committee determined that the thesis is acceptable in form and content and that a satisfactory knowledge of the field covered by the thesis was demonstrated by the candidate during an oral examination. A signed copy of the Certificate of Approval is available from the School of Graduate and Postdoctoral Studies.

Abstract

Remote Canadian communities rely on diesel generators for their electricity needs. Providing such generators with fuel year-round presents challenges because of inclement weather and long transportation distances involved. This work presents the conceptual design of a 10 MWth microreactor that can be used to provide district heating and 3.5 MW of electricity to remote communities. The reactor has a lead-cooled and graphite-moderated core with 13 vertical fuel channels containing 10 wt% enriched HALEU fuel. The core is enclosed in a non-pressurized reactor vessel and is passively cooled through natural convection. Stirling engines are used to drive the electrical generators. The hot cylinders of the Stirling engines are located in the unpressurized reactor vessel and are heated directly by the primary molten lead coolant. Preliminary neutronic and thermal-hydraulic analyses of the core indicate that the design is technically feasible and that the reactor can function for two years and nine months without refuelling.

Keywords: microreactor; lead cooled; graphite moderated; stirling engine

Author's Declaration

I hereby declare that this thesis consists of original work of which I have authored. This is a true copy of the thesis, including any required final revisions, as accepted by my examiners.

I authorize the University of Ontario Institute of Technology (Ontario Tech University) to lend this thesis to other institutions or individuals for the purpose of scholarly research. I further authorize the University of Ontario Institute of Technology (Ontario Tech University) to reproduce this thesis by photocopying or by other means, in total or in part, at the request of other institutions or individuals for the purpose of scholarly research. I understand that my thesis will be made electronically available to the public.

Statement of Contributions

I hereby certify that I am the sole author of this thesis. The general reactor concept described in this thesis has been developed with advice from the thesis supervisor. The description of the ZAN4e Reactor has been submitted for publication in a technical journal. I have used standard referencing practices to acknowledge ideas, research techniques, or other materials that belong to others. Outside of what was described above, I hereby certify that I am the sole source of the creative works and/or inventive knowledge described in this thesis.

Acknowledgements

I would like to give my deepest appreciation to Dr. Eleodor Nichita who supported and believed in me since meeting him at the beginning of my nuclear engineering undergraduate degree. He has been an inspiring mentor by providing guidance and direction in my pursuit of developing and designing a nuclear microreactor. I attribute the majority of what I know about reactor design to him. I would like to thank Ontario Tech University for providing the program to learn and instill in me a strong appreciation for nuclear physics, the engineering design process, nuclear safety culture, and the pursuit of excellence. I also want to thank the Canadian Natural Sciences and Engineering Research Council for supporting this work through a Discovery Grant.

I could not have undertaken this journey without my wife, Macey, who with her strength and continual optimism, supported and encouraged the pursuit of my dream of a better energy future. She was a remarkable sounding board to test out my ideas, and I could not have done it without her.

I am extremely grateful for my extraordinary parents, Kathy and Eric, for raising me to have a questioning attitude, to pursue excellence, to work on meaningful things to make the world a better place. I want to thank my sisters, Lindsay and Hannah, who were always their to keep me grounded and focused on what is most important. I want to thank my grandparents, Karen and Gordon, who have been examples of discipline and hard work for me in my life. I also want

to thank all of my family and friends for their love, support, and encouragement throughout the development of this work. I would have given up long ago if it was not for that support.

Special thanks to the mentors in my life who collaborated with me on the ideas in this research, helped me see things that I was missing, and for extending my vision of what is possible. The list of individuals who fall in this category is extensive, but to acknowledge a few, thank you Dan and Regan Bickman, Elaine Hartrick, Darrel Aunger, Regan Davis, Aaron Nardella, John and Linda Kehgias, and Brent Thomas.

Finally, words cannot express my gratitude for Suzanne West, my incredible aunt, who was a remarkable business woman, leader, and engineer. She was the woman who inspired me to become a nuclear engineer so I could find a better way to bring clean and reliable energy to the world that would be beneficial for the planet, people, and profits. Without her example, vision, and counsel, I would not be where I am today.

Contents

List of Tables

List of Figures

List of Abbreviations and Symbols

CFD	Computational Fluid Dynamics
CNSC	Canadian Nuclear Safety Commission
HALEU	High-Assay Low-Enriched Uranium
INAC	Indigenous and Northern Affairs Canada
LNG	Liquid Natural Gas
LMFBR	Liquid Metal Fast Breeder Reactors
MHD	Magnetohydrodynamic
MSR	Molten Salt Reactor
MWt	Megawatt Thermal
MWe	Megawatt Electrical
NRCan	Natural Resources Canada
PHWR	Pressurized Heavy Water Reactor
RCED	Remote Communities Energy Database
SMR	Small Modular Reactor
SWR	Sodium Water Reaction
TRISO	TRistructural ISOtropic

Chapter 1

Introduction

1.1 Background

Most Canadian arctic communities use Diesel generators as their main source of electrical power since they are not connected to any major electricity grids. According to the Remote Community Energy Database (RCED) [1], as of 2018, there were approximately 280 communities (equating to about 200,000 people) in Canada that fall under the definition of "off-grid" or "remote" (terms can be used interchangeably) [2]. To be termed as "off-grid" or "remote," the community must not be connected to the North American electrical grid nor to the piped natural gas network, and it must be a permanent or long-term settlement (5 years or more) with at least ten dwellings [3]. Figure 1.1 shows a map of the RCED with all the locations across Canada that meet the classification of off-grid or remote. The different-coloured dots in Figure 1.1 represent the primary power source for the community, with most communities relying on diesel power (red dots and triangles). The other energy sources shown in Figure 1.1 are heavy fuel oil (purple), hydro (blue), natural gas (black dots and triangles), other fuel sources that are fossil fuel based (yellow), local grid fossil fuel connections (green), and

unknown energy sources (grey). Of the off-grid communities, approximately 78% rely on fossil fuels, 9% are connected to a provincial/territorial grid (producing electricity via fossil fuels or hydro), and 13% use hydro to generate their energy needs [1]. Currently, no remote community is utilizing renewable energy as their primary power source. The total percentage of remote communities in Canada that are relying on fossil fuel-based power generation, including those connected to a provincial/territorial grid, is greater than 78%. Moreover, almost all communities that use hydro as their primary energy source rely on backup diesel power generation to supplement production during peak energy demand or to provide power during outages [2].

The main issues of relying on diesel power generation in remote communities are that diesel has high transportation and operating costs, high emissions relative to other types of power generation, and its price can be very volatile [4]. In addition, significant subsidies are required to help keep energy affordable for these remote communities [2].

Steering remote communities away from fossil fuel based sources and toward alternative energy-generating options does not come without its challenges, such as [5]:

- Extreme weather conditions making it difficult to use solar and/or wind.
- Long, expensive, and seasonally unreliable transportation routes.
- Unpredictable diesel and Liquid Natural Gas (LNG) prices.
- Aging infrastructure and high upfront capital replacement costs.
- Limitations of technical expertise in emerging clean technologies.
- Debt caps.
- Growing demand for electricity with limited new generation options.

Figure 1.1: Remote and off-grid communities in Canada [1].

- Political and regulatory pressure to keep electricity rates low.
- Limited customer base.

Another option that has been proposed to reduce fossil fuel reliance in remote communities is to install more transmission lines to connect remote communities up to the North American electrical grid. However, installing more transmission lines to connect remote communities to the North American electricity grid could cost millions of dollars per km in construction costs alone. In addition, the cost of operations, maintenance, construction of transmission stations, and the purchase or leasing of land for transmission lines will raise the cost of electricity for end users [6].

Based on the RCED, the average fossil fuel generating capacity of a remote arctic community in Canada is approximately 3.6 MWe, while the median generating capacity is 1.4 MWe [1]. However, when looking at the communities relying on fossil fuels, it can be observed that communities have the majority of their installed generating capacity in the lower capacity range compared to the higher range. When tallying up the generation capacity for each of these communities into discrete generation capacity ranges, Figure 1.2 shows that 238 of the 276 (i.e., 86.2%) remote communities have a generation capacity of less than, or equal to, 3.5 MWe. Figure 1.3 shows a more detailed distribution of communities with less than, or equal to, 3.5 MWe of installed fossil fuel generation capacity. Figure 1.2 and Figure 1.3 indicate that the design and development of a 3.5 MWe nuclear microreactor would service the most remote communities.

A recent study by Natural Resources Canada, in collaboration with provincial and territorial governments, found the price of unsubsidized electricity in remote arctic communities to be as high as \$1.14/kWh, approximately ten times higher than the rates of \$0.10-0.15/kWh in high-population centres which are connected to the main electricity grid [7]. The bulk of the price differential comes from

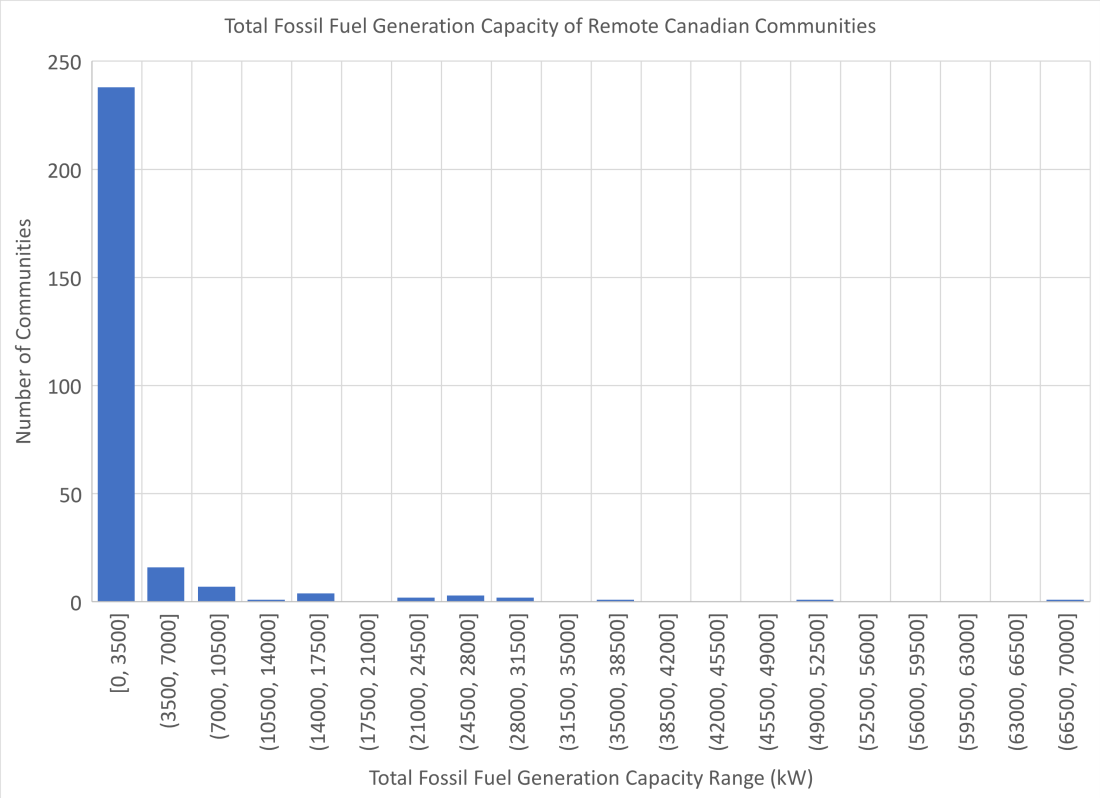

Figure 1.2: Total fossil fuel generation capacity distribution of Remote Canadian communities (created from available RCED data [1]).

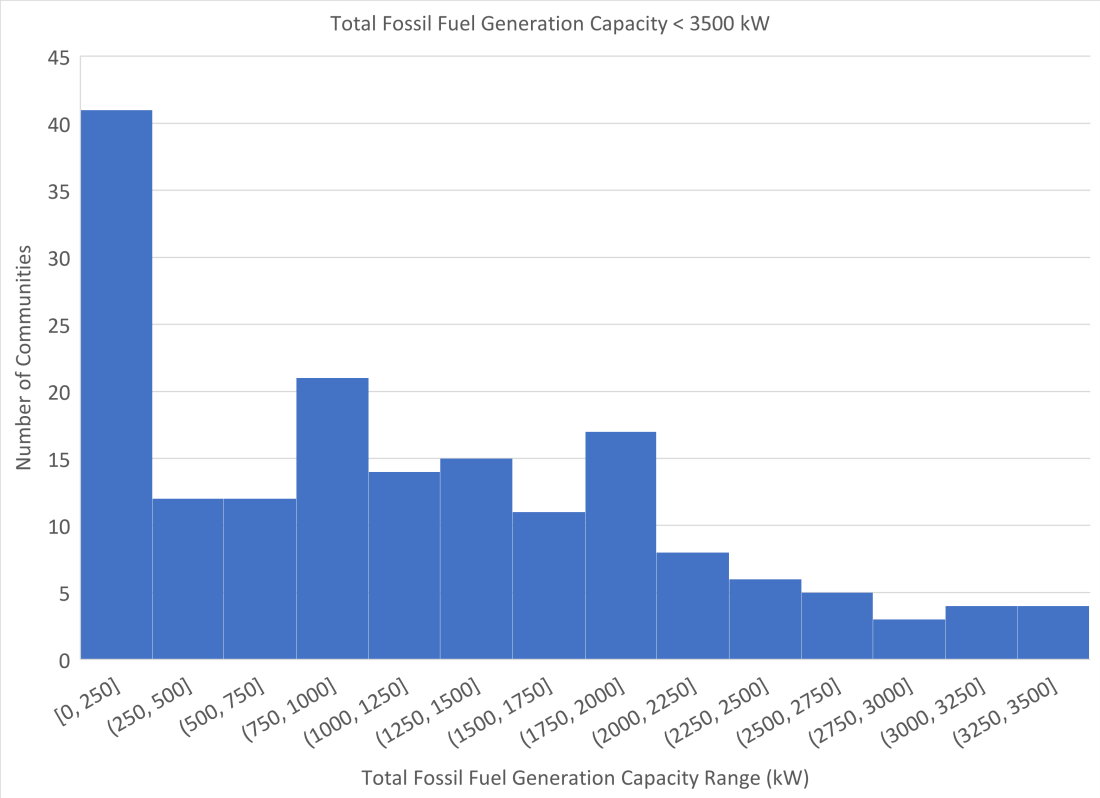

Figure 1.3: Fossil fuel distribution of Remote Canadian communities with less than, or equal to, 3500 kW of installed generation capacity (created from available RCED data [1]).

fuel transportation costs, storing large quantities of fuel on-site, and maintaining aging infrastructure. It is, therefore, desirable to replace diesel generation with a much higher energy density source, such as nuclear generation.

1.2 Objective

The work outlined in this thesis has two main objectives:

1. Develop a conceptual design for a microreactor that is adequate for remote Canadian Arctic communities.

2. Demonstrate that the proposed microreactor design satisfies basic functional and safety requirements.

1.3 Scope

The scope of this thesis predominantly focuses on the reactor physics of the nuclear microreactor, with basic thermal-hydraulic models to support the conceptual design. The requirements that are focused on in this thesis are the functional and safety requirements outlined in Table 1.1.

1.4 Requirements of a reactor for remote communities

Canadian Arctic communities are not adequately served by current Diesel generation systems. A system based on a nuclear microreactor (1-20 MWt) could provide a better solution, however, a reactor for small arctic communities needs to satisfy a number of requirements, which are outlined in Table 1.1. The requirements are categorized as follows (letters in parentheses show abbreviations used

in the table): Functional (F), Performance (P), Safety (S), and Environmental (E). The requirements that were addressed in the most detail are F1, F2, S1, S2, and S3.

Table 1.1: Design requirements of microreactor for remote/off-grid communities.

ID	Requirement	Justification
F1	Shall be able to offer electricity as well as central heating for arctic communities.	Many of the arctic communities rely on diesel fuel for both heat and electricity. The reactor solution needs to be able to provide both.
F2	All structures, systems, and components of the reactor shall be enclosed in a single containment structure that can be transported as one unit.	This will support transportation and reduce the demands on setup, construction, and commissioning.
P1	Shall have an electrical output of approximately 3.5 MWe, corresponding to the power capacity needs of the majority of arctic communities.	According to the Remote Communities Energy database for Canada [1] the majority of households have power less than or equal to 3.5 MWe.
P2	Shall be transportable by ship, train, plane, or truck.	Many of Canada's remote communities are only accessible by a certain means of transportation during certain parts of the year.

Continued on next page

Table 1.1: Design requirements of microreactor for remote/off-grid communities. (Continued)

ID	Requirement	Justification
P3	Shall not exceed 72,500 kg.	This is the maximum payload mass allowable by the CC-177 Globemaster III transport plane owned by the Royal Canadian Air Force [8].
P4	Shall have dimensions less than 26.82 m (88 ft) in length and 3.76 m (12.33 ft) in diameter.	These are the maximum dimension constraints of the CC-177 Globemaster III loading bay [8].
P5	Shall be able to last at least two years without having to be refueled.	A two-year fueling cycle is the average fueling cycle that LWRs utilize and this should allow sufficient time to procure and transport the fuel to site.
P6	Reactor shall maintain structural integrity in temperatures as low as -75°C.	The reactor will be sited in very cold and harsh environments and needs to be able to withstand them.
P7	Coolant shall not expand when freezing.	Due to the reactor being placed in cold environments, it is vital that the coolant doesn't cause damage to SSCs if it were to freeze.

Continued on next page

Table 1.1: Design requirements of microreactor for remote/off-grid communities. (Continued)

ID	Requirement	Justification
P8	Shall have fuel enrichment less than 20 wt% U-235 to avoid difficulties with sourcing enriched fuel.	Anything over 20 wt% fuel will start to cause problems in sourcing it, as well as in the safeguards and regulatory space.
S1	Coolant shall not have a volatile reaction with wator or air.	Due to the reactor being in arctic communities, that are surrounded by large amounts of water, it is vital that the coolant is not reactive with water.
S2	Shall operate at atmospheric pressure.	With the reactor operating in a remote region where emergency response is lacking, it is desirable to have enhanced safety features so that the probability of an accident is reduced.
S3	Shall employ natural convection cooling in the core.	An important feature of Generation IV reactors is the use of passive safety features, such as natural convection cooling. This will also reduce the need for complex engineered safety systems to ensure sufficient core cooling.

Continued on next page

Table 1.1: Design requirements of microreactor for remote/off-grid communities. (Continued)

ID	Requirement	Justification
E1	Shall be able to be removed from the operation site without any permanent damage to the local environment.	Many of these remote communities only have a few hundred people in them. It would be unwise for a microreactor sited at these locations to have a detrimental and long-lasting negative effect on the environment.

Chapter 2

Potential Application of Reactor Technologies and Systems

This chapter presents a review of existing and proposed reactor technologies that satisfy at least some of the criteria in Table 1 and that could potentially be used for powering a small Arctic community.

2.1 Technologies

This section is broken down into the four main technology areas that define a Nuclear Power Reactor System: neutron spectrum, type of fuel, type of coolant, and heat-to-work conversion system.

2.1.1 Neutron Spectrum

The neutron spectrum is an important characteristic of any Nuclear Reactor System. The two main types of neutron spectrum are fast and thermal. Figure 2.1 shows two generic neutron energy spectra for fast and thermal reactors, with the fast reactor having a higher neutron flux at higher energies compared to a thermal

reactor.

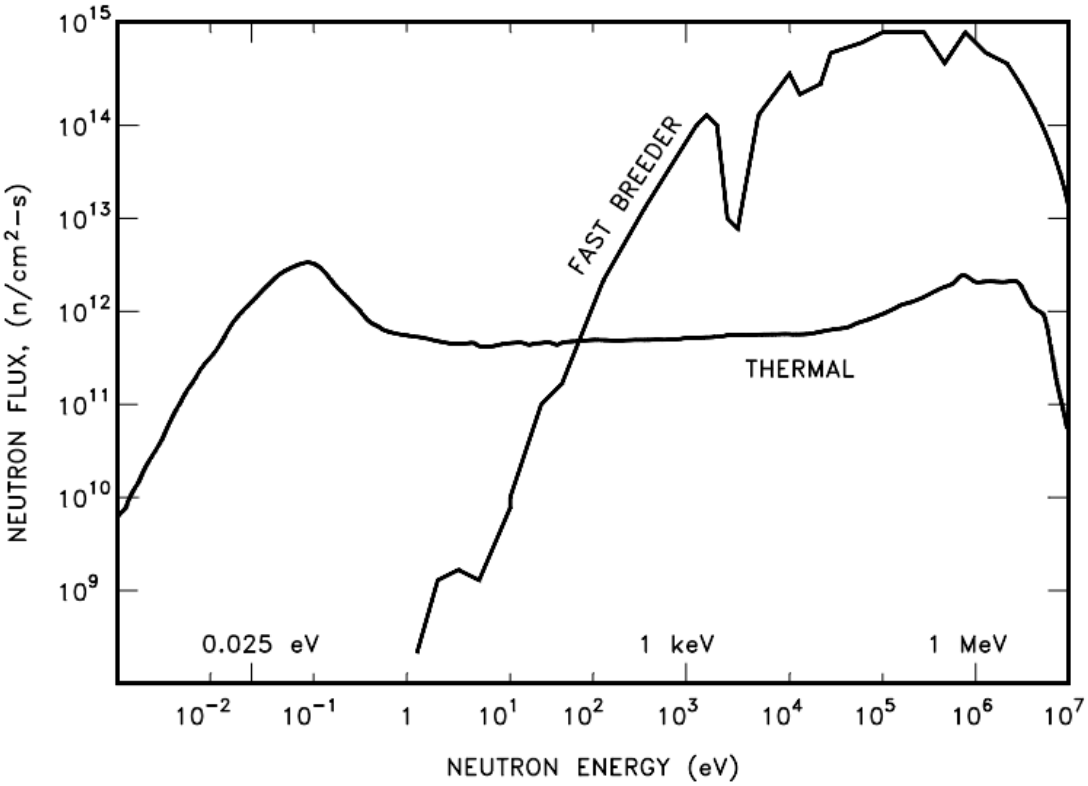

Figure 2.1: Comparison of generic neutron spectra for fast and thermal reactors [9].

Fast Neutron Spectrum Reactors

In a fast reactor, the fission chain reaction is sustained by neutrons that have energies between 1 MeV and 10 MeV, with the majority being about 5 MeV [10]. Corresponding velocities are well above $9 \times 10^6 m/s$ (≈3% the speed of light). The high energy neutrons in fast reactors allows for the fissionable but non-fissile U-238 to be fissioned, as well as to breed an excess of Pu-239, compared to thermal reactors. Due to U-238 having a larger absorption cross-section with higher energy neutrons, compared to thermal energy neutrons, Pu-239 is able to be bred and burned in the core, thus extending fuel resources [11]. In a fast reactor, the core typically will consist of a Pu-239 and U-235 fuel, which drives the majority of

heat generation in the core, and is surrounded by a blanket of depleted or natural uranium to be converted to Pu-239 by absorption of fast neutrons [12, p. 179]. No neutron moderator (i.e., heavy water, light water, or graphite) is used in fast reactors to keep the neutron energy high.

As outlined by the Generation IV International Forum, the use of a fast neutron spectrum supports extensive recycling of fuel as well as supports breeding fissile fuel from fertile material in hopes of producing "equal or more fissile material than the reactor consumes" [13, p. 8]. Fast-neutron spectrum reactors reduce the quantity of nuclear waste compared to thermal spectrum reactors. However, fast reactors require larger amounts of neutron shielding compared to thermal reactors due to the large neutron leakage in fast reactors. Fast reactors also require more engineered safety systems due to the fact that a fast reactor can go prompt critical faster than a thermal-neutron spectrum reactor [14, p. 349]. More complex control systems are also needed due to no delayed neutrons helping to control the reactor like in a thermal-spectrum reactor [14, p. 349]. As shown in Figure 2.2, the fission cross section for U-238, a fissionable material, increases markedly above approximately 1 MeV.

Thermal Neutron Spectrum Reactors

In a thermal reactor, the fission chain reaction is sustained by neutrons that have energies of about 0.025 eV and velocities of 2200 m/s. Getting a neutron down to this speed after it is emitted from fission requires a moderator to slow it down to thermal energies. Neutrons are typically born with an average energy of approximately 2 MeV, and then the moderator that is present in the core will slow the neutron energy down to thermal energies (0.025 ev). Figure 2.3 shows that the slower the neutron energy, the higher the probability of fission to occur. Fissile materials such as U-233, U-235, and Pu-239 behave in his manner.

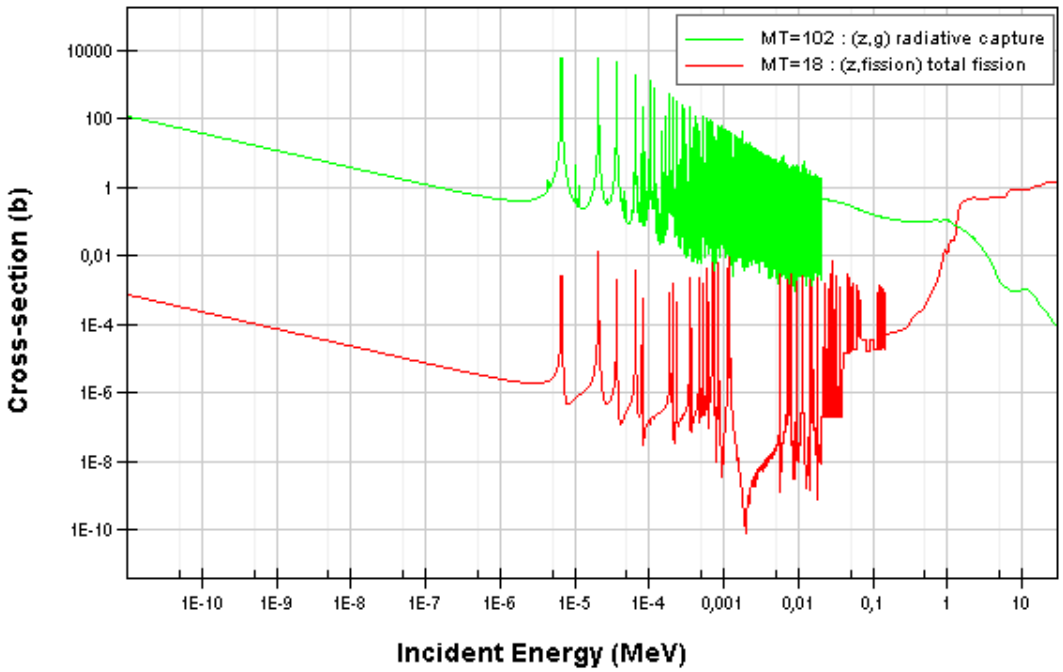

Figure 2.2: Total fission and radiative capture cross-sections for U-238 (taken from [15] and recreated from ENDF/B-VII.1 Nuclear Data Library).

Thermal neutron reactors will also breed some Pu-239, but unlike fast reactors a thermal reactor is not optimized for the breeding of additional fissile isotopes such as Pu-239. A thermal energy spectrum has been predominantly used in reactor designs today due to them being slightly easier to control compared to fast reactors [14, p. 349].

2.1.2 Fuel

Uranium Dioxide

Uranium dioxide is part of the ceramic fuel category and is what is predominantly used in nuclear power reactors today due to its high melting point (2850°C), excellent irradiation stability, high neutron utilization, exceptional corrosion resistance, compatibility with cladding and ease of manufacturing [16, p. 177]. However, some of the disadvantages of UO_2 fuel include the fact that it has low thermal

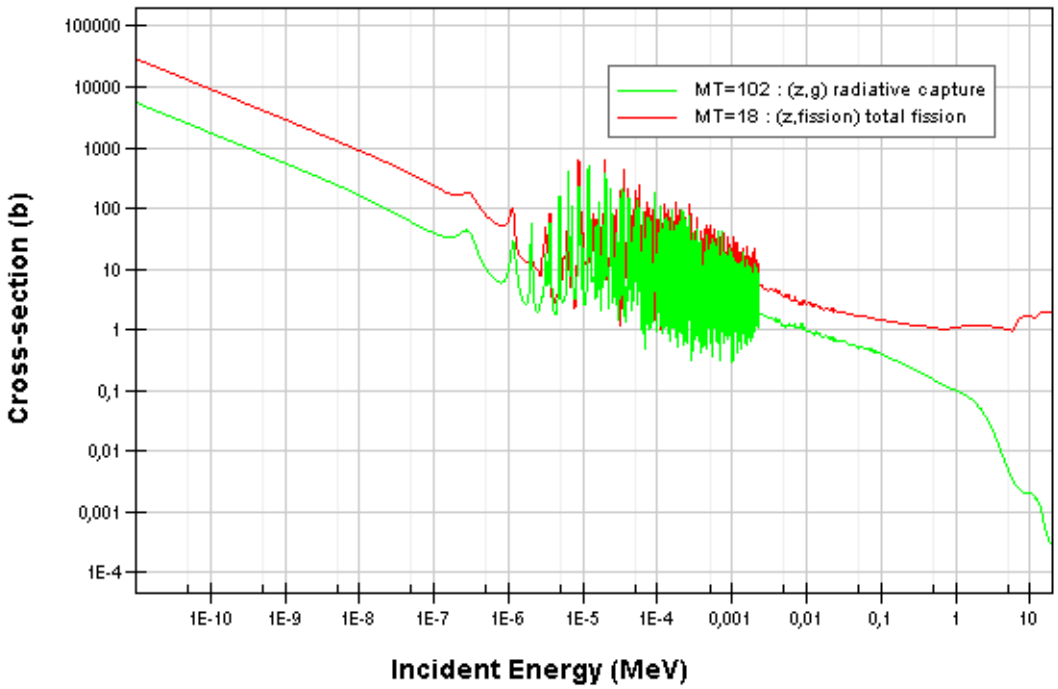

Figure 2.3: Total fission and radiative capture cross-sections for U-235 (taken from [15] and recreated from ENDF/B-VII.1 Nuclear Data Library).

conductivity, poor thermal shock resistance and relatively low fissile atom density (compared to metal fuels). The low thermal conductivity in the UO_2 fuel results in a very steep temperature gradient across the fuel pellet, which can result in the fuel centerline temperature being much higher than the outer surface temperature. This can lead to the non-uniform distribution of pores, oxygen concentration, and fission products in fuel pellets [16, p. 177].

Metal Fuels

The appeal of metal fuels is that they have the ability to provide higher thermal conductivity and a higher fissile density. These two factors will help to compensate for the neutron penalty that will need to be paid when using new cladding materials that have higher absorption cross sections [16, p. 180]. By using a metal fuel which has a higher fissile density, it allows for the fuel cycle length to be extended and the core lifetime to last longer without having to be refuelled.

However, a major disadvantage of metal fuels is their low melting point, their slightly worse irradiation induced swelling compared to ceramic fuels like UO_2, and their higher chemical reactivity with coolants such as water [16, p. 180].

TRISO Fuel

The type of fuel that High-Temperature Reactors (HTR) often leverage, due to the high-temperature environment, is TRistructural-ISOtropic particles (TRISO). TRISO particles typically consist of five regions/layers (see Figure 2.4) [17]:

1. Fuel region: kernels of oxide (UO_2), carbide (UC), or oxycarbide (UCO) fuel that are typically micrometres in diameter.

2. Carbon buffer: a porous layer of carbon which serves to attenuate the recoiling fission fragments and accommodate the gas buildup from the fission products.

3. Inner pyrolytic carbon layer (IPyC): protects SiC layer from chemical attack.

4. Silicon carbide (SiC) layer: acts as the main pressure vessel for the fuel.

5. Outer pyrolytic carbon layer (OPyC): protects SiC layer from chemical attack.

The interest in TRISO particle fuel is that it is known for its excellent fission product retention capabilities, as described in 1 through 5 above, when placed in a high-temperature gas cooled environment [16, p. 182]. As it relates to the Generation IV reactors that are being investigated, HTRs are on the list of the six major reactors of interest [18]. The use of TRISO fuel in HTRs supports the Safety and Reliability goals for Generation IV Nuclear Energy Systems, which include the following [18]:

- **Safety and Reliability-1**: Generation IV nuclear energy systems operations will excel in safety and reliability
- **Safety and Reliability-2**: Generation IV nuclear energy systems will have a very low likelihood and degree of reactor core damage
- **Safety and Reliability-3**: Generation IV nuclear energy systems will eliminate the need for offsite emergency response.
- **Proliferation Resistance and Physical Protection-1**: Generation IV nuclear energy systems will increase the assurance that they are very unattractive and the least desirable route for diversion or theft of weapons-usable materials and provide increased physical protection against acts of terrorism.

Potential challenges of TRISO fuel include the fact that there has been little to no operating experience in North America (potential licensing risk) and that the manufacturing process of the TRISO particles/fuel is fairly unique and novel. A TRISO-fuelled reactor requires the use of hundreds of thousands of TRISO particles. As a result, fuel fabrication will be required to have a high level of reliability and reproducibility. It is also much more difficult to identify all of the defective particles as they cannot be removed until the process is complete, and the large number of particles that would need to be inspected could be very burdensome from a cost and schedule perspective [19, p. 57]. Despite the strong fission retention of TRISO fuel, the possibility of fuel failure and the release of fission products outside of the sphere is plausible and has happened in situations such as at the German AVR reactor. The AVR reactor also showed that temperatures can become higher than predicted and can result in fission product release into the core [20].

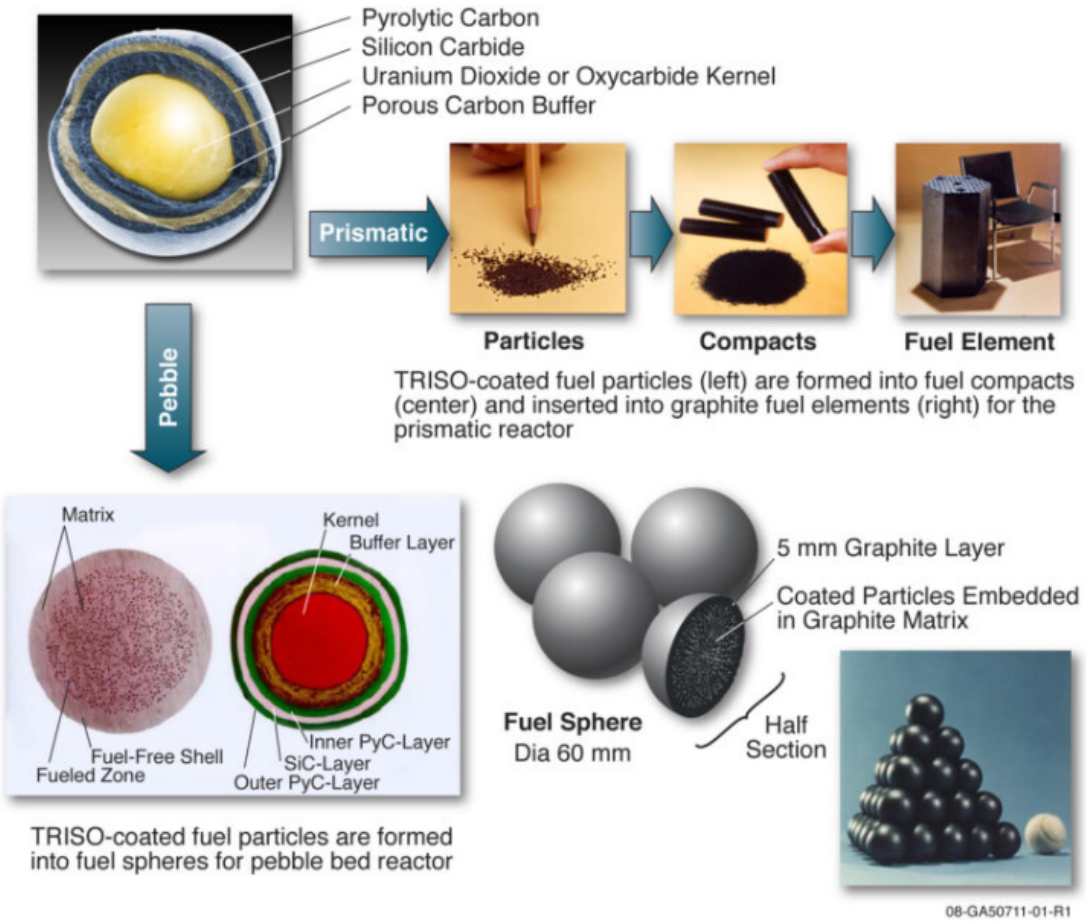

Figure 2.4: TRISO particles in Pebble and Prismatic configurations. Taken from a presentation given by Andrew Sowder and Cristian Marciulescu from EPRI [21].

Molten Salts

A Molten Salt Reactor (MSR) mixes the coolant and fuel into a homogeneous mixture, which presents a few distinct advantages and disadvantages. Potential advantages of MSRs include fuel reprocessing without shutting the reactor down, reduced complexities of fabricating solid fuel, spent fuel can be reduced as it can be used as an input fuel, and better utilization of the fuel due to higher levels of achievable burnup [22].

Other major advantages arise due to the fact that the coolant and the fuel are combined in a homogeneous mixture. These advantages include [23]:

- "Meltdown" becomes an irrelevant term due to the fact that the fuel and coolant are already liquid.
- There is little to no heat transfer delay due to the fuel being part of the coolant.
- There is no need to have a loading or fuel management plan as the fuel is homogeneous with the coolant.

Some of the major disadvantages that arise from the use of MSRs that make them unfeasible for a remote Canadian Arctic community include:

- the need for exotic materials to protect the reactor structures, systems, and components from salt corrosion that would dramatically increase the price of a microreactor [22].
- additional engineered safety systems needed to deal with Tritium that is produced within the reactor, due to most baseline salts containing lithium [24].
- Chemical reactions of the molten salt with air and water [22].

The use of an MSR is of interest for larger cities that are looking for hundreds of MW of electricity. There have been very few designs that use a molten salt coolant or MSR for the purposes of a microreactor.

2.1.3 Coolant

Water

The use of water as a coolant has a lot of operating experience in the nuclear industry and is a great coolant material to use in nuclear reactors. However, Generation IV reactors do not use water as a coolant, and its use should be avoided in reactors in the Canadian Arctic due to the positive volume coefficient water has when it freezes. When water freezes, its volume increases in size, which in turn would greatly impact piping and component integrity in the event of a reactor trip or shutdown and the water coolant were to freeze due to extreme cold conditions in the Canadian Arctic.

Sodium

The use of sodium-cooled reactors in the Canadian Arctic has the major downfall in that sodium has a "strong chemical reactivity with oxygen and water, producing a sodium fire or sodium-water reaction (SWR)" [25]. This is a serious concern given the fact that the reactors that will be designed and built for these remote communities will be surrounded year-round by potentially large quantities of water (vapour, liquid, and ice). Another concern that many SMR designers have with sodium cooled SMRs is that it needs to have an intermediate coolant loop to "avoid aggressive chemical reaction of radioactive sodium in the primary circuit with water that is supplied" to a generation turbine [26]. Even though SWRs can be mitigated with the use of early leak detection measures or by reducing the number of connection pipes and branching, the risk of an SWR is too high of a

risk [27, p. 110].

Of the ten current Generation IV metal-cooled designs outlined by the IAEA, only two of them are sodium cooled, and the rest are lead cooled. Even though the likelihood of a SWR can be reduced significantly, the consequence of an SWR event makes it worthwhile to pursue other reactor coolants to be used for a reactor in the Canadian Arctic.

Lead

The use of lead as a coolant presents a wide array of advantages, which include [28], [29]:

- Has excellent cooling properties, while maintaining little to no absorption of neutrons.
- High boiling points, eliminating the issue of dry-out or void coefficients.
- Can be operating at atmospheric pressure due to its high boiling point.
- Inertness to air and water.
- Has a very high density which gives it the ability to perform natural convection cooling for normal operation without the complexities that come from water.
- No hydrogen production like what occurs with water cooled reactors.
- Has a high retention of fission productions.

Even though lead-cooled reactors fall into the same category as sodium-cooled reactors (i.e., liquid metal cooled reactors), they eliminate the need for an intermediate coolant loop, thus decreasing design complexity and capital cost while still leveraging the benefits of increased heat transfer capabilities and operating at atmospheric pressure [26, p. 4].

When it comes to lead-cooled reactors, the two candidate coolant compositions that are being considered in advanced reactors are lead-bismuth eutectic (LBE), typically with a make-up of 44.5 wt% Pb + 55.5 wt% Bi, and pure lead (Pb) [30, p. 127]. Using just Pb as the coolant can come in either natural lead, which is composed of various isotopes of Pb, or a single isotopic form of Pb such as Pb-208. The use of Pb-208 as the coolant is very beneficial as it has the lowest neutron absorption cross-section of all the Pb isotopes [31]. The advantage of LBE versus Pb is that LBE has a melting point of 123.5°C, while Pb has a melting point of 327°C. The boiling points of each are relatively close, where LBE is 1670°C, and lead is 1740°C [29]. The use of LBE is cheaper than Pb; however, the use of LBE results in the production of Po-210 through the activation of Bi-209 followed by beta decay [30, p. 27]. The presence of Po-210, a very toxic alpha emitter, would require specific engineered systems to manage it [30]. The overall disadvantages of using LBE include the need for a chemical treatment loop to clean the coolant, the considerable decay heat that is produced from Po-210 ($\approx$140 W/g), and the high radiation risk from Po-210 that is posed to humans [30, p. 250].

Based on the Technology Roadmap Update for Generation IV Nuclear Energy Systems from 2014, there are three main concerns around lead cooled reactors that a lot of R&D money is being spent to move the technology forward [32]. These include:

- Materials corrosion: due to the high temperature of the flowing lead, exotic steels and coatings need to be used to avoid corrosion and erosion.
- Core instrumentation: the opacity of the lead makes it very difficult to inspect and monitor the in-core components.
- Seismic/structural issues: due to the weight of the lead within the reactor vessel, it presents seismic and structural challenges.

One of the major advantages of lead coolants is their increased heat transfer characteristics compared to water, organic, and gas coolants. They can also be advantageous for their low moderating properties, which makes them very compatible with fast reactors. What makes lead coolants so appealing for Generation IV reactors is that they are particularly resistant to radiation damage, have relatively low melting points and high boiling points, and allow for high reactor exit temperatures with low system pressures [33, p. 259-261].

There are two things that need to be considered when looking at the use of metal coolants in a reactor [33, p. 259]:

- High neutron absorption cross-sections
- Supply chain and cost

Lead coolants have low neutron absorption cross sections in the high and intermediate energy ranges. However, the neutron absorption cross section starts to increase for some lead coolants in the thermal energy range, which can pose an issue for thermal reactors [33, p. 259]. As shown in Figure 2.5, the capture cross-section decreases as the incident neutron energy increases. As it relates to lead coolants, Figure 2.5 also shows that Pb-208 has the lowest capture cross sections across the thermal and epithermal energy range. Graphite is the typical moderator to be used in lead cooled reactors and is shown in this figure as a comparison of how the capture cross-sections of the different lead isotopes compare to the graphite moderator that will also be present in the core. The graphite moderator is more likely to capture neutrons, and the lead coolant would be almost "invisible" to the neutrons.

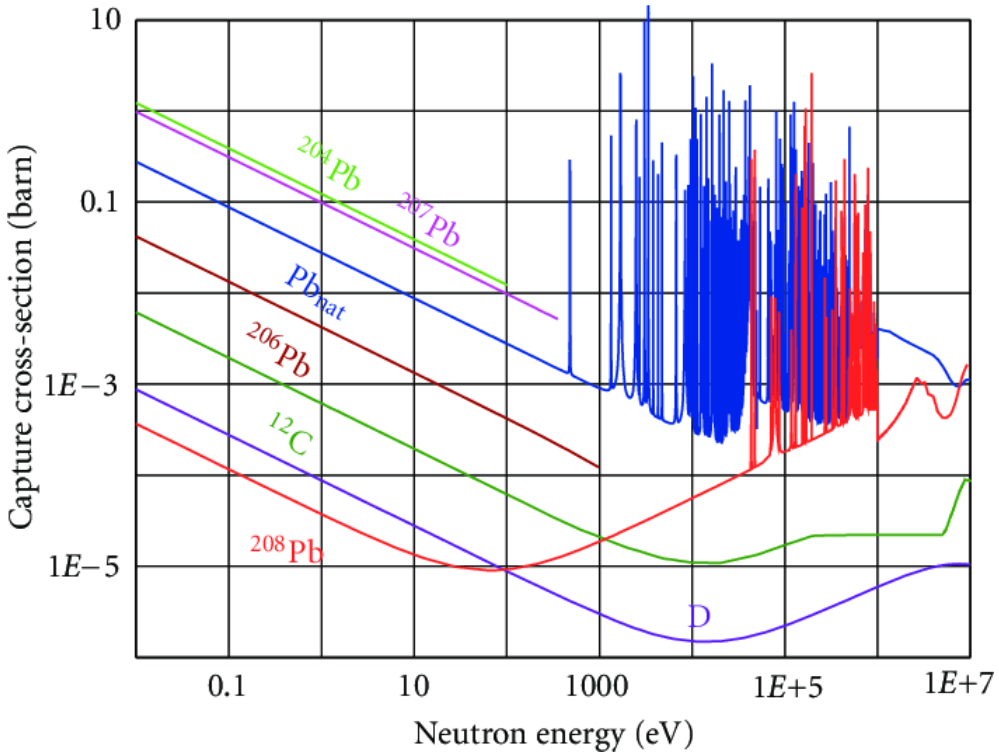

Figure 2.5: Capture cross-section of various lead isotopes and carbon [34]

2.1.4 Heat Conversion Systems

In most operating nuclear power plants, the heat that is generated through the fission of fuel in the reactor is used to produce steam, which can occur directly inside the reactor or in auxiliary heat exchangers that are called steam generators [14, p. 132]. This combination of the reactor and steam generator is typically called the Nuclear Steam Supply System (NSSS). The steam that is produced in the NSSS is then used to drive large turbines, which are connected to generators for conversion to electricity. The use of a steam turbine generator set is a very traditional way of converting the heat from fission to electricity and is shown in Figure 2.6. Steam comes in from the NSSS and drives the High-pressure and Low-pressure turbines. The rotation of these turbines, in turn, drives the electrical generator (top right) to produce electricity, as shown in Figure 2.6 [14, p. 133].

With the advent of SMRs and nuclear microreactors, the use of a steam turbine

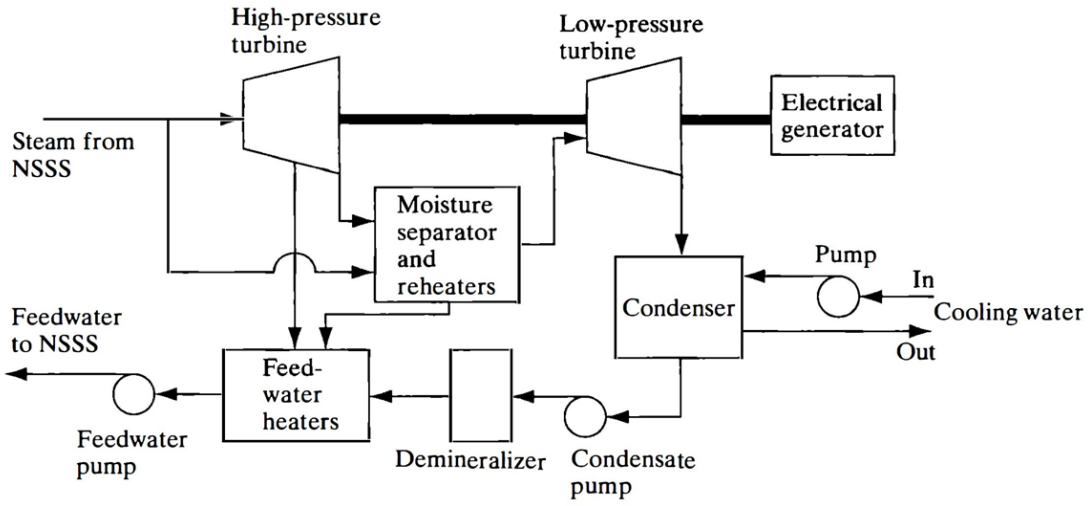

Figure 2.6: Layout of a typical steam turbine generator set [14, p. 133]

generator set is possible if small turbine generator sets are used. However, with highly advanced fuel and coolant options being proposed, the use of alternative heat to electricity conversion systems has become a topic of investigation. Specifically, technologies that can convert heat to electricity using a single loop (direct cycle) configuration are of interest. These include options such as Thermoelectric Converters, Stirling Engines, and Magnetohydrodynamic Generators (MHD). The use of direct heat to electricity technology is prevalent in remote and isolated locations, such as space, where maintenance or replacement of a secondary loop between the reactor and the turbine is not feasible. The use of thermoelectric converters, Stirling engines, and MHDs have all been used in space reactors and have the potential of being used for the direct heat to electricity conversion in a microreactor for remote/off-grid communities [35].

Stirling Engines

The use of Stirling engines is a solution that is elegant and very feasible. A Stirling Engine (SE) uses a cycle comprising isothermal compression and expansion and constant volume heating and cooling, as shown in Figure 2.7. A major advantage

of Stirling Engines is that there is no internal combustion, and the engine runs on an external heat source which gives it the flexibility in the environment it can be placed. A second advantage is that they are reversible engines in that the hot side can become the cold side and vice versa. As a third advantage, SEs run on a closed loop cycle, so the working gas is not released and does not need continual refuelling.

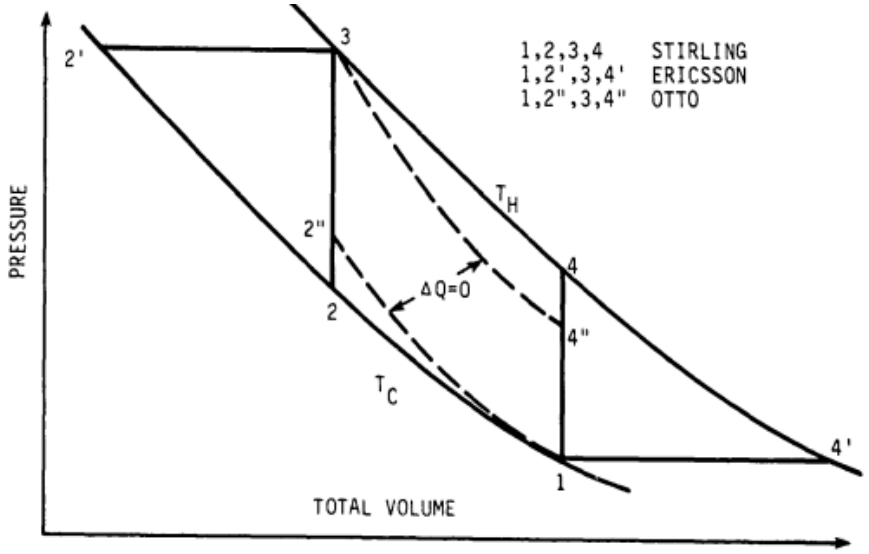

Figure 2.7: Theoretical Stirling, Ericsson, and Otto Cycles (taken from [36, p. 61])

There has been plenty of research performed on space reactors to use Stirling engines [35]. The U.S. Department of Energy has spent large amounts of money on researching Stirling Engine designs [36]. There are dozens of designs that have been tested in laboratories across the US and have the potential to be utilized with a nuclear reactor [36, p. 12-59, 399–409]. Many of the designs originated from the interest in replacing the combustion engine in cars with a Stirling engine.

Like any combustion engine, the Stirling engine goes through the four processes of compression, heating, expansion, and cooling, as shown in Figure 2.7. Of the Stirling engine designs, there are three different types: Alpha, Beta, and Gamma, as shown in Figure 2.8 [36].

Of the three different types of Stirling engines, the Alpha type engine is the

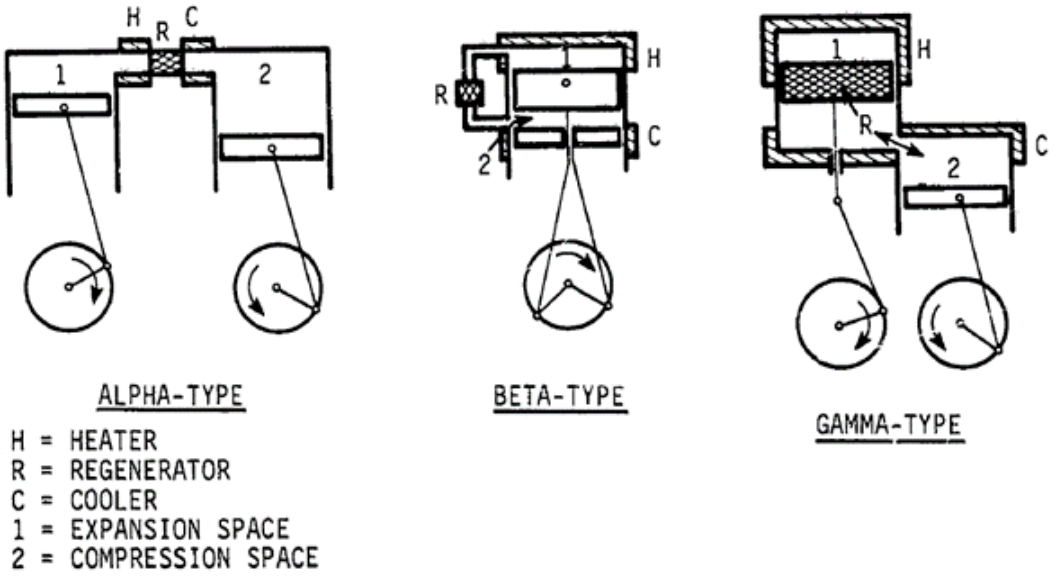

Figure 2.8: Three different Stirling engine types (taken from [36, p. 9])

simplest type to design, as well as model, considering that there is a clear separation between the hot and cold cylinders. Alpha type Stirling engines also have the advantage that they don't have any early mixing that might occur in a beta or gamma type engine [37]. The advantages of the beta and gamma type configurations is due to their ability to take up less space from their smaller designs [38].

Of the three different types of Stirling Engines (i.e., α, β, and γ), the γ-type Stirling Engines produce the most power and are more efficient when compared to the other two Stirling Engine types [39]. However, for the purposes of reactor design, the equations governing a dual piston SE (i.e., alpha configuration) are typically used due to their lower performance, and thus is a more conservative approach than using the more efficient γ-type Stirling Engine equations.

The nomenclature for engine internal volumes and motions are shown in Figure 2.9 and 2.10. A description of each of the symbols shown in Figure 2.9 are outlined in Table 2.1. Figure 2.10 shows an additional view of the basic structure of a beta-type Stirling Engine. The left side of Figure 2.10 that is coloured red is the

effective hot gas temperature, T_H, and the right side that is coloured blue is the effective cold gas temperature, T_C.

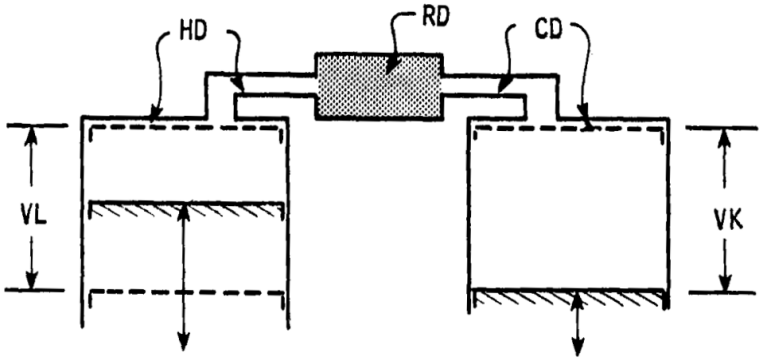

Figure 2.9: Dual piston engine nomenclature and high-level schematic [36, p. 82]

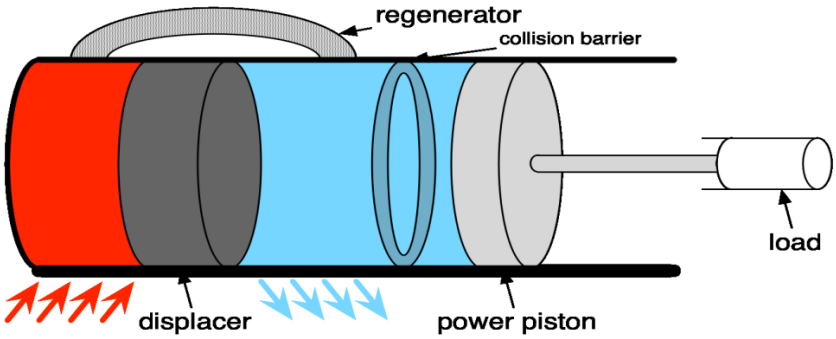

Figure 2.10: Basis structure and components of a Stirling Engine [40]

The following equations govern the volumes and pressures for analyzing a given Stirling engine geometry and were sourced from [36].

Hot Volume as a function of crank angle,

$$H(N) = \frac{VL}{2}[1 - sin(F)] + HD \tag{2.1}$$

Cold Volume as a function of crank angle,

$$C(N) = \frac{VK}{2}[1 - sin(F - AL)] + CD \tag{2.2}$$

Total Volume as a function of crank angle,

$$V(N) = H(N) + C(N) + RD \tag{2.3}$$

Engine Pressure as a function of crank angle,

$$P(N) = \frac{MR}{\frac{H(N)}{TH} + \frac{C(N)}{TC} + \frac{RD}{TR}} \tag{2.4}$$

Table 2.1: Symbols, definitions, and units for Equations 1, 2, 3, and 4

Symbol	**Definition**	**Units**
HD	Hot dead volume	cm^3
RD	Regenerator dead volume	cm^3
CD	Cold dead volume	cm^3
VL	Hot piston live volume	cm^3
VK	Cold piston live volume	cm^3
TH	Effective hot gas temperature	K
TC	Effective cold gas temperature	K
TR	Effective regenerator gas temperature, $TR = \frac{TH-TC}{ln(TH/TC)}$	K
M	Engine gas inventory in moles	mol
R	Gas constant	8.314 J/mol·K
AL	Phase angle	90°

The equation that governs the work per cycle,

$$W1 = (PX)(VT)\frac{\pi(1-AU)}{(K+1)}\left(\frac{1-DL}{1+DL}\right)^{1/2}\left(\frac{DLsin(ED)}{1+(1-(DL)^2)^{1/2}}\right) \tag{2.5}$$

A description of each of the symbols in equation 2.5 is shown in Table 2.2.

Table 2.2: Nomenclature symbols, definitions, and units for equation 2.5

Symbol	**Definition**	**Units**
W1	Work per cycle	Joules
PX	Maximum pressure during cycle	MPa
VT	$VL + VK = (1+K)VL$	cm^3
K	Swept volume ratio $= VK/VL$	dimensionless
AU	TC/TH	dimensionless
DL	$\frac{\left[(AU)^2+2(AU)(K)cos(AL)+K^2\right]^{1/2}}{AU+K+2S}$	dimensionless
S	$S = \sum_{s=1}^{s=n} \frac{(V(S))(TC)}{(VL)(T(S))}$ Where V(S) and T(S) are the volumes and absolute temperatures of the dead spaces.	dimensionless
RV	Dead volume ratio, VD/VL	dimensionless
VD	Total dead volumne $= HD + RD + CD$	cm^3
ET	$ET = tan^{-1}\left(\frac{Ksin(AL)}{AU+Kcos(AL)}\right)$	dimensionless

There are many companies across North America and Europe that have designed, developed, and constructed Stirling Engine designs that are available on the commercial market. Some prominent companies include Genoastirling (Italy), Azelio (Sweden), Sunpower Inc. (USA), and Qnergy (USA). The general parameters of each are shown in Table 2.3. Figures of the TES.POD 1.0, ML3000, and

PCK80 are also shown in Figure 2.11, Figure 2.12, and Figure 2.13.

Table 2.3: Parameters of Azelio, Genoastirling, and Qnergy Stirling engines.

	TES.POD 1.0 (Azelio)	**ML3000 (Genoastirling)**	**PCK80 (Qnergy)**
Electrical power generated	13 kW	Up to 3.3 kW	Up to 7.1 kW
Gas used	Not disclosed	Nitrogen	Nitrogen
Output duration	13 hours/day	24/7	24/7
Electrical efficiency	Not disclosed	14%	30%
Working Temperature	600°C	850°C/950°C (hot side)	400°C to 800°C
Starting Temperature	Not disclosed	700°C (hot side)	Not disclosed
Rotation per minute	Not disclosed	(with load) up to 750	Not disclosed
Cooling	Water	Water (from 4.5 up to 6.4 L/min)	Water (20 to 40 L/min)
Weight	1000 kg	250 kg	250 kg

Heat Pipes

Heat pipes are a simple two-phase flow heat transfer device that are able to efficiently transfer heat from liquid to vapour, with very little losses, between evaporator and condenser with high effective thermal conductivity. They are a closed evaporator-condenser system that consists of a sealed, hollow tube, whose

Figure 2.11: TES.POD 1.0 by Azelio. Taken from Azelio website [41].

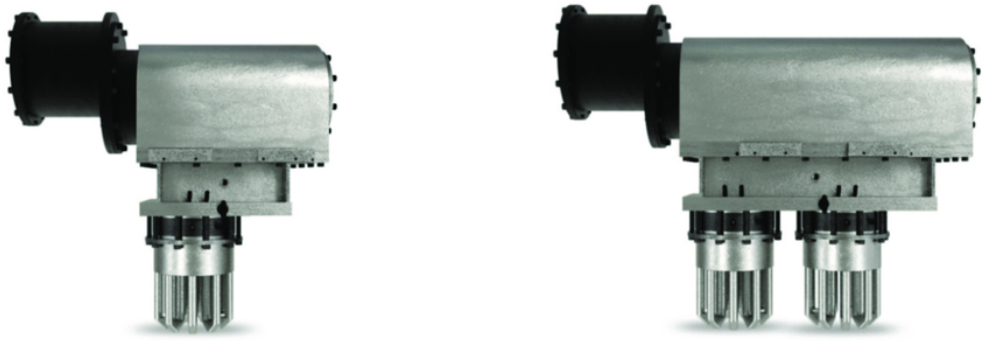

Figure 2.12: ML1000 (left) and ML3000 (right) by Genoastirling. Taken from [42].

Figure 2.13: Power Conversion Kit (PCK) 80 made by Qnergy. Taken from Qnergy website [43].

inside walls are lined with a capillary structure or wick [44, p. xxv]. A high-level concept is shown in Figure 2.14, where when heat is applied to any portion of the heat pipe evaporator section, it will cause the liquid to evaporate and fill the center region of the heat pipe. The heat is then transferred out via the heat sink at the condenser location, and the vapour filling the center region becomes a liquid again and flows towards the evaporator section via capillary forces along the outside wick structure [44, p. 4].

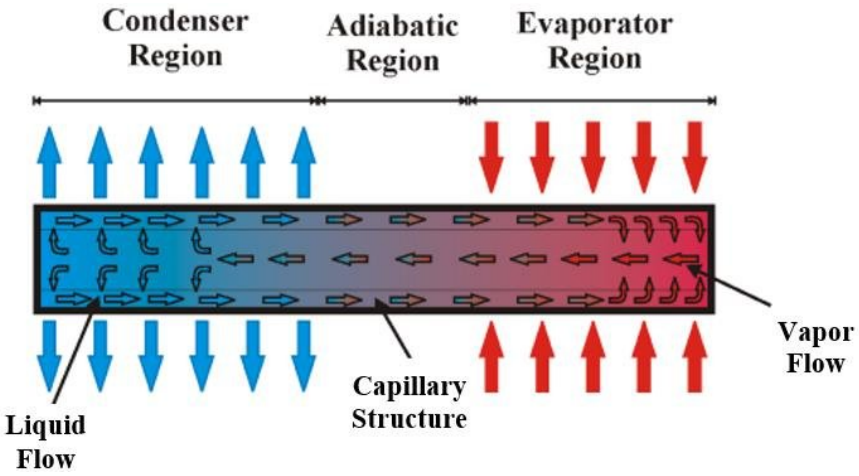

Figure 2.14: Heat pipe concept with flow path [45].

The working fluid in heat pipes can vary depending on the application, ranging from cryogens to liquid metals [44, p. 5]. For applications in a nuclear reactor, the use of a liquid metal for the working fluid is typically chosen. There are several major benefits of heat pipes, which include [44, p. 28]:

- For a comparable weight and size heat transfer method, heat pipes have a much higher heat transfer capability.
- Heat pipes allow for flexibility in terms of where they can be placed for removing heat.
- Very little heat loss over long distances.
- Requires no external power to operate.

Despite their major advantages, heat pipes are not immune to drawbacks, which can include [44, p. 27-32]:

- Incompatibility between the wall structure and working fluid can lead to corrosion and gas formation.
- Demanding maintenance and cleaning requirements to avoid residual contamination that can lead to gas formation.
- Transmutation of working fluid will result in contamination which cannot be filtered out. Regardless of the fluid, the minimum purity of the working fluid must be at least 99.999%.
- Operating in below freezing temperatures can result in the working fluid temperature dropping and cause the vapour pressure of the fluid to drop off. This allows for noncondensable gases that are created by contamination to expand and can create pumping and pressure problems in the pipe.
- Dry-out risks due to the two-phase flow of the working fluid [46].
- Heat pipe failure in the reactor core results in temperature rises and stress concentrations and can result in cascade heat pipe failures [47].

There are two microreactors that are currently being developed in the US that use heat pipe technology to ensure that the reactor core is kept well below the melting point and transfers heat out of the core. The eVinci reactor is being developed by Westinghouse, and the Aurora reactor is being developed by Oklo.

Magnetohydrodynamic Generators

A Magnetohydrodynamic (MHD) Generator generates electricity directly from the moving stream of an ionized fluid that flows through a magnetic field [48]. As shown in Figure 2.15, as the ionized fluid (red line) flows through the magnetic

field (grey line), an electric current is produced due to the induced voltage (blue line).

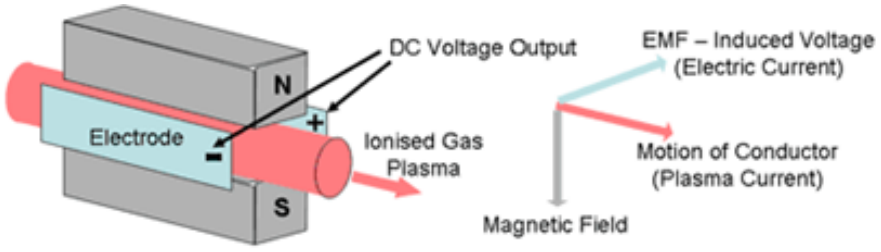

Figure 2.15: Magnetohydrodynamic Power Generation Principle [49].

In a nuclear application, the coolant would need to be a gas such as He or Xe. The reactor would then need to be designed in such a way to ensure that the He/Xe gas is ionized as it leaves the reactor core. This ionized gas would then create an induced voltage as shown in Figure 2.15.

NASA has been one of the largest researchers into the feasibility and effectiveness of using MHDs with a nuclear reactor in space [50], [51], [52]. MHDs have a lot of potential as it allows for a larger electrical output for smaller amounts of weight. Figure 2.16 shows a proposed schematic of an MHD coupled with a nuclear reactor for space applications [53].

The University of Florida has also looked at coupling an MHD with a vapour or gas core reactor. Instead of using solid state fuel as shown in Figure 2.16, the fuel would be in the form of UF_4 gas that is mixed with an ionizing gas such as a helium and xenon mixture. As a result, the coolant gas and fuel would be a homogeneous mixture of gases, leveraging a similar idea as MSRs. Most MHD coupled nuclear reactors would be limited by the solid fuel-cladding temperature (approximately 1850°C for Zr-4 [54]). However, with a vapour core reactor coupled with an MHD allows for much higher operating temperatures, on the order of 2500 K and higher [55], as there is no physical components that would be at risk of melting. The UF_4 fueled system mixed with He/Xe as the working fluid, with a

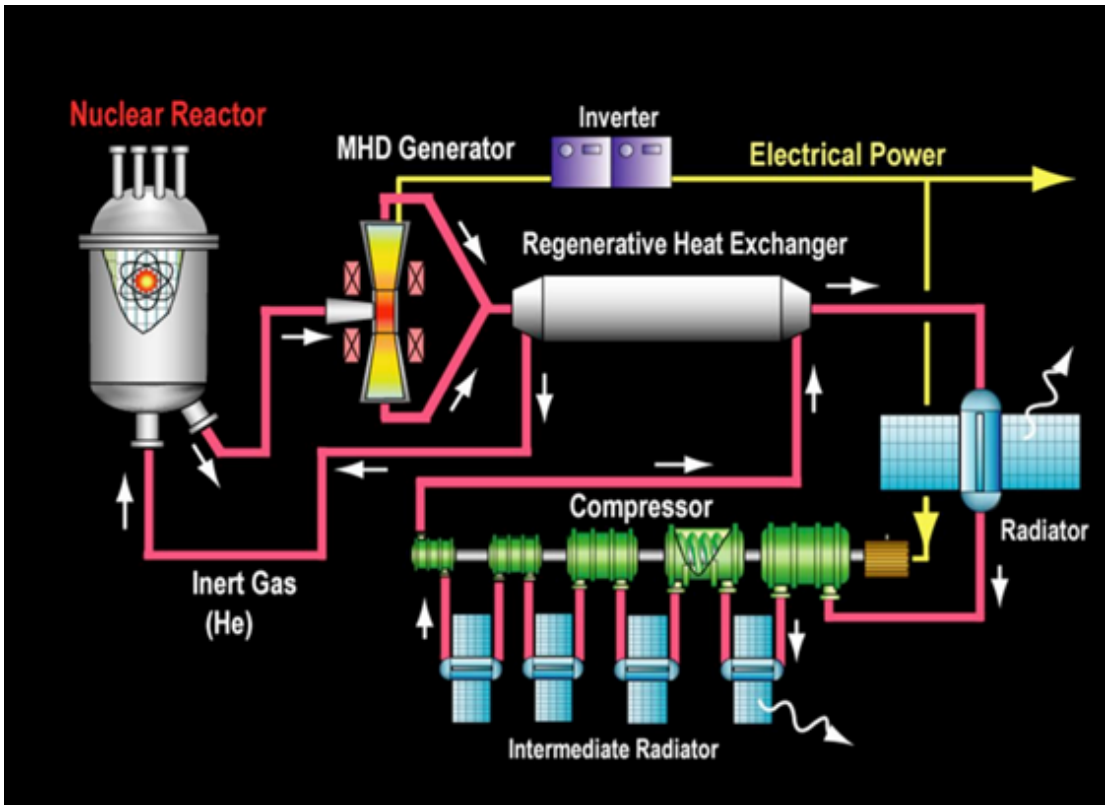

Figure 2.16: Schematic of closed cycle MHD with a nuclear reactor [53]

closed loop MHD cycle, directly processes and converts the fission power between temperatures of 1800 to 3000 K [56]. Mixing the gases UF_4 with He/Xe is a very elegant way of converting heat to electricity, and with 10% enriched uranium in the UF_4 the closed cycle MHD is capable of obtaining efficiencies as high as 55%. Figure 2.17 shows a conceptual schematic of the VCR and MHD coupled design.

2.2 Reactor Systems

This section focuses on the actual reactor system designs that exist and that employ one or more of the four technology categories discussed in Section 2.1. The two main categories of reactor systems that are of interest to this review include Small Modular Reactors (SMRs) and microreactors, due to the heat and electricity requirements of remote Canadian communities being significantly less

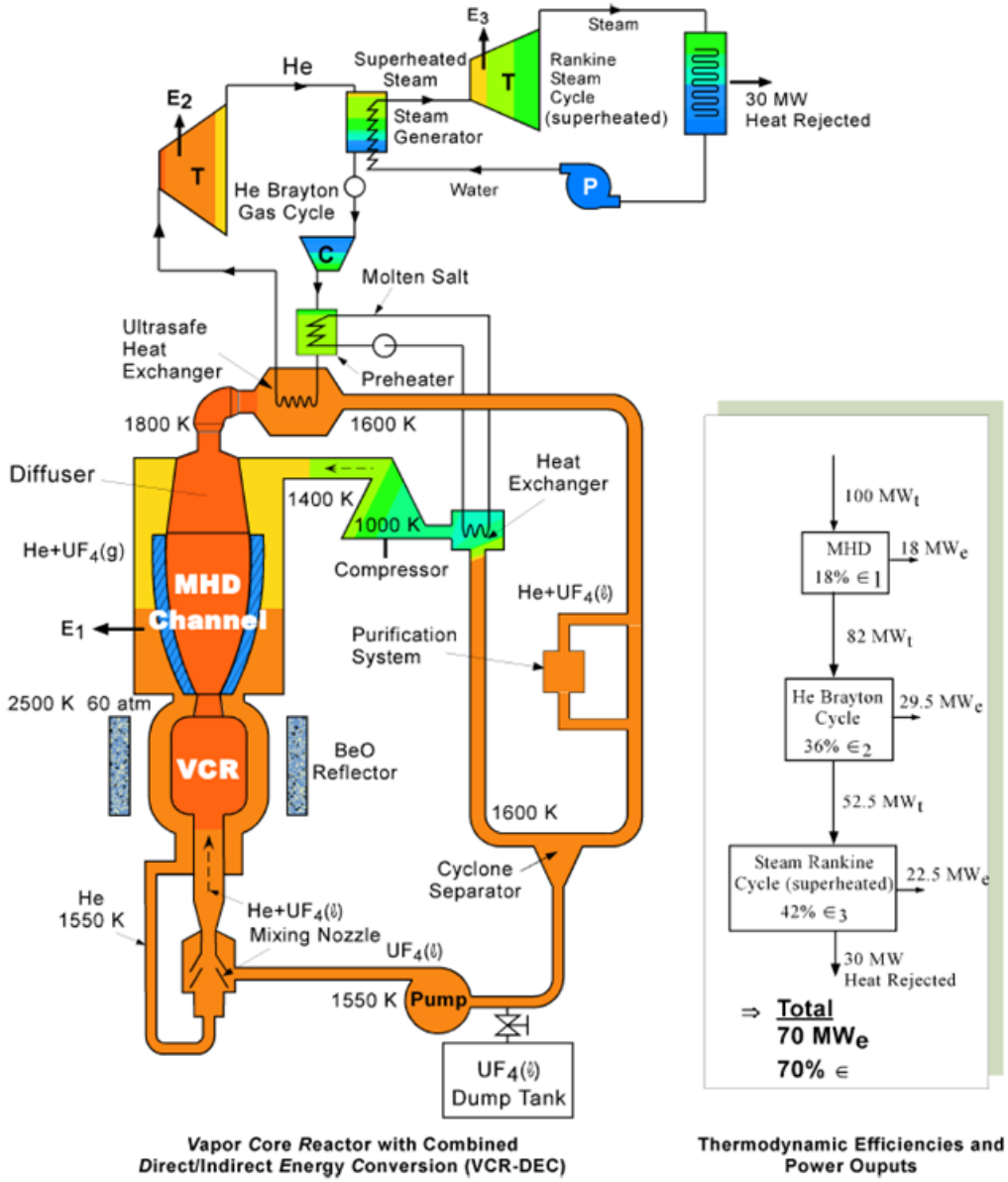

Figure 2.17: Schematic of a Vapour Core Reactor (VCR) coupled with an MHD [56]

than 300 MWe. SMRs and microreactors are the primary types of reactors that are potentially the most relevant for such small remote Canadian communities due to their suitable thermal/electrical capacity, and their modular design features making it easier for transportation and construction. The Canadian Nuclear Safety Commission (CNSC) defines a small reactor facility or SMR as "a reactor facility containing a reactor with a power level of less than approximately 200 megawatts thermals (MWt) that is used for research, isotope production, steam generation, electricity production or other applications" [57]. Microreactors are usually understood to have thermal powers below 20 MWt [58].

This review focuses on SMRs and microreactors that satisfy some of the general requirements outlined in Table 1.1, in particular systems that use non-water based coolants (due to the volume increase of water upon freezing), that use coolants which are inert in air and water, and that are factory fabricated and easily transportable. Systems that require little to no on-site operators due to their incorporation of "Inherent" and "Passive" safety design features are of particular interest as well. Inherent safety in the design means that a specified hazard is eliminated due to the incorporation of a specific material and/or design concept into the design [59, p. 5]. For example, the use of a low-pressure coolant like lead eliminates the hazard of high-pressure coolants existing in the plant and removing the need for a robust pressure boundary. Passive safety means the design incorporates structures, systems, and components that require no external input to operate and rather rely on natural laws, properties of materials, and internally stored energy to ensure safety in the design [59, p. 5]. An example of passive safety in the design would be the use of natural convection to cool the reactor rather than the use of forced convection pumps. Figure 2.18 shows the comparison of current SMR and microreactor designs from various companies and their electrical output [60].

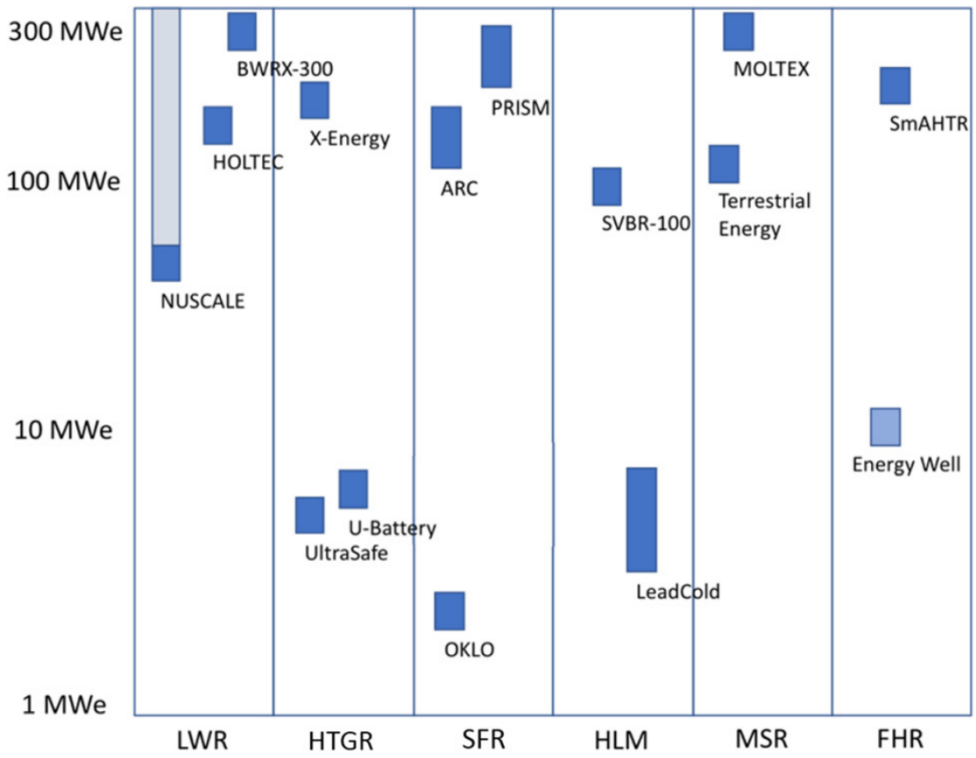

Figure 2.18: Comparison of electrical capacity (MWe) of various SMR and microreactor designs [60].

Of the Generation IV reactors that are being proposed, the non-water-based coolant reactors that are being investigated for potential use in a remote Canadian community include gas-cooled reactors, sodium-cooled reactors, molten salt reactors, and lead-cooled reactors.

2.2.1 ARC-100 (ARC Nuclear Canada, Inc.)

The prominent sodium cooled SMR design that exists today is the ARC-100 by ARC Nuclear Canada, Inc. The ARC-100 is a non-pressurized liquid Sodium cooled Fast Reactor (SFR) that produces 286 MWt and 100 MWe via 13.1 wt% enriched metal fuel (U-Zr-alloy). Due to the fast neutron spectrum that it uses, it is able to consume its own waste as it is developed in the core, which allows the refuelling cycle to extend to 20+ years. Its core inlet and outlet temperature are 355°C and 510°C, respectively. For its power conversion system, it leverages

the use of a Rankine steam cycle turbine [61, p. 201-204].

ARC-100 has some desirable features for application in remote Canadian communities, such as:

1. Utilizes inherent reactor safety with passive, diverse, and redundant decay heat removal.
2. Only needs to be refuelled every 20 years.
3. High outlet temperature to support district heating.
4. Successful operating experience from EBR-II.

The use of sodium is less desirable for use in the Canadian Arctic as the volatility of molten sodium with water can be catastrophic, as outlined in Section 2.1.3. Its physical dimensions also make it very prohibitive for transportation, where its height and diameter are 15.6 m and 7.6 m, respectively. Due to its dimensions, the set up of the ARC-100 in a remote community would require it to be shipped in several modular pieces, which may make construction complicated and time consuming. The thermal and electrical capacity are also much larger than what is actually needed in the majority of remote Canadian communities.

2.2.2 Integral MSR (Terrestrial Energy Inc., Canada)

The IMSR is a low-enriched (<5 wt%) graphite moderated molten fluoride fuel salt reactor that produces 440 MWt and 195 MWe. It utilizes forced circulation to maintain a coolant inlet and outlet temperature of 620°C and 700°C, respectively. It is called an "integral" MSR because it is a completely sealed reactor vessel with the pumps, heat exchangers, and shutdown rods all mounted within a single vessel. The entire sealed core-unit is replaced after approximately seven years with a new core module [61, p. 201-204]. The main advantages of the IMSR include:

1. The reactor core is never opened up to replace fuel, the entire core unit is replaced.

2. It was specifically designed for factory fabrication, and due to its core life being approximately 7 years it allows for factory production levels of quality control and economy.

3. Strong operating experience based on the Molten Salt Reactor Experiment (MSRE).

4. Fissile materials achieve very high levels of burnup as there is no worry of fuel failure since the fuel is already a liquid.

5. Strong load following capability due to intermediate salt loop heat exchanger.

The IMSR is a Generation IV design that is better suited for a medium to large city. Even though only one unit can produce 195 MWe, the power plant is designed to accommodate at least two core units for replacing core units with little to no downtime. Thus, the plant will produce at least 390 MWe, which is far more electrical capacity than any remote Canadian community will need.

2.2.3 Stable Salt Reactor (SSR) - Wasteburner (Moltex Energy)

The SSR developed by Moltex is designed for countries that have large quantities of spent nuclear fuel. It is a molten salt reactor, but it isn't like typical molten salt reactors where the fuel and coolant are homogeneously mixed. Rather, the design is based on Moltex's patented concept of containing the fissile molten salt in vented tubes whilst using a different molten salt as the primary coolant. There are two configurations of the SSR. There is the SSR-Wasteburner (i.e., SSR-W)

as well as the SSR-Uranium (i.e., SSR-U). The SSR-W is a fast reactor that uses recycled waste as fuel, while the SSR-U is a uranium-fueled, thermal spectrum reactor which generates heat at higher temperatures [62]. The SSR-W is the "flagship" design for Moltex, while the SSR-U is still in the conceptual design phase. The SSR-W is fueled with reactor grade plutonium that is recycled from stocks of spent uranium oxide fuel [61, p. 263]. The spent uranium oxide fuel that is sourced from various reactors such as LWRs, AGRs, and CANDUs is converted to reactor grade plutonium via the WAste To Stable Salt (WATSS) facility.

The SSR-W is a 750 MWt and 300 MWe reactor that utilizes a molten salt $ZrF_4 - KF$ coolant. It runs on an inlet and outlet temperature of 525°C and 590°C, respectively. The advantages of the SSR-W include:

1. It is able to recycle large quantities of spent nuclear fuel and convert it into a usable form via the use of WATSS.

2. It has the major advantages of a MSR without the contamination of fission products in pumping equipment and other components along the coolant flow path.

The disadvantages of the SSR-W include the fact that the SSR-W needs to be directly connected with a WATSS facility which makes siting requirements more complicated and restrictive. It is more feasible to have the SSR-W as close as possible to already operating LWR, AGR, or CANDU plants to accept spent fuel for recycling. In addition, the other disadvantage that makes this an unfeasible reactor for the Canadian Arctic is how much complex chemistry is going on in this reactor. It will require a highly skilled and competent individual to be available to deal with any issues that may arise. This may pose difficult if the SSR-W were to be located in a remote Canadian location.

2.2.4 Energy Well (Czech Republic)

Energy Well is of the most interest as it has an electrical capacity that is close to that needed to power remote Canadian communities. The Energy Well reactor is a fluoride high-temperature pool type reactor that utilizes FLiBe as its molten salt coolant. The fuel type that it utilizes is TRISO fuel compacts that are enriched to 15 wt%. It produces 20 MWt and 8 MWe, with a core inlet and outlet temperature of 650°C and 700°C, respectively [63]. The Energy Well reactor is a molten salt cooled reactor, but it is not a molten salt fueled reactor. The TRISO fuel and FLiBe coolant are not homogenous. Like the IMSR, the Energy Well reactor also has a lifetime of approximately seven years, after which it is placed in a cooldown bay of the power plant and a new reactor unit is brought in to replace the previous one. The Energy Well utilizes a unique energy conversion system by leveraging super critical carbon dioxide. It uses an Ericsson-Brayton cycle configuration to transform the heat into electricity and is able to do it at efficiencies >42% [60].

The advantages of the Energy Well reactor include:

1. It utilizes the robustness of TRISO fuel with the high heat transfer capabilities of a molten salt.

2. Utilizes a unique energy conversion system that maintains a high efficiency while still allowing it to be small and easily transportable.

3. It utilizes a small site footprint (<4000 m^2).

The Energy Well reactor may be one of the best solutions for use in remote Canadian communities. However, it is not an ideal solution due to it using primary, secondary, and tertiary cooling circuits. For a remote Canadian location, the reactor needs to utilize as few pumps, moving parts, and engineered systems as possible to avoid cascading failures, ensure a high level of reliability, and reduce the need for maintenance.

2.2.5 STARCORE (StarCore Nuclear)

The STARCORE reactor is a High-Temperature Gas Cooled Reactor (HTGR) that is helium cooled, graphite moderated, and fueled with 15 wt% TRISO fuel prismatic compacts. The STARCORE reactor is very scalable, ranging from 14 MWe all the way up to 360 MWe. HTGR reactor systems are of potential interest to use in remote Canadian communities. However, due to the operating pressure being 7.4 MPa on the primary side and 6.7 MPa on the secondary side, this does not meet the intended design requirement of being able to operate at atmospheric pressure [61, p. 141-144]. The other disadvantage is the lack of operating experience with TRISO fueled reactors in Canada, as outlined in Section 2.1.2.

An advantage of StarCore is that it meets all the remote siting requirements, which include: inherently safe, passively secure, has load following capability, is fully automated, has remote shutdown (intervention) capability, and after some qualification, can be operated with a zero-radius exclusion zone [61, p. 142]. Another advantage of StarCore is the fact that it owns the Intellectual Property of a modern fully automated control system design called the StarCore Automated Reactor System (STARS) HyperVector Control System [61, p. 143]. It was previously used in many aerospace systems and has been independently reviewed by the former Atomic Energy Canada Limited (AECL) as well as Canadian National Laboratories (CNL) [61, p. 143]. The StarCore plant can be completely monitored or shutdown remotely at all times via satellite links, which is a major advantage for remote Canadian communities as it would not require personnel to be onsite at all times.

2.2.6 Xe-100 (X-energy, LLC)

The Xe-100 is a HTGR that is helium cooled, graphite moderated, and fueled with 15.5 wt% TRISO fuel pebbles. It utilizes online fuel loading and has a core inlet and outlet temperature of 280°C and 750°, respectively. The Xe-100 is a 200 MWt and 82.5 MWe reactor. This reactor design is a Generation IV reactor that utilizes a TRISO fuel form that is incredibly robust and able to retain its fission products in almost all circumstances. However, the Xe-100 size and electrical capacity far exceeds what most remote Canadian communities need. HTGR reactor systems are of potential interest for use in remote Canadian communities, however, due to the operating pressure being 6.0 MPa on the primary side and 16.5 MPa on the secondary side, this does not meet the intended design requirement of being able to operate at atmospheric pressure [61, p. 175-178].

The main advantage of the Xe-100 is its ability to use online refuelling, which allows it to achieve very high burnup per fuel pebble to help reduce the quantity of highly radioactive fission products that would typically take hundreds of thousands of years to decay. The Xe-100 is made to provide effective load following capabilities as well as to produce high-temperature steam for process heat applications, which would be very advantageous for smaller communities [61, p. 175-178]. Its load following capabilities can go from 100% full power to 40% full power within just 20 minutes. In addition, this is one of the only reactor designs that is capable of partnering with renewable energy sources in a sustainable way due to its load following capabilities [64]. X-energy is also developing its own fuel fabrication facility called TRISO-X. This is a major advantage as it eliminates the supply chain issue of TRISO fuel for the Xe-100 [65].

The disadvantages of the Xe-100 are similar to what is captured in Section 2.1.2 relating to TRISO fuel. The other disadvantage is its large thermal and electrical capacity. The Xe-100 was not indented to be built for remote commu-

nities. Rather, its target market is replacing fossil fuel power plants in large cities across North America.

2.2.7 Micro Modular Reactor (UltraSafe Nuclear Company)

The MMR is a HTGR that is helium cooled, graphite moderated, and fueled with 19.75 wt% TRISO fuel that produces 15 MWt and 5 MWe. It has a core inlet and outlet temperature of 300°C and 640°C, respectively [61]. The MMR is a reactor system that is of particular interest for use in remote Canadian communities due to its electrical capacity being very close to what a large number of remote communities need. It also employs passive cooling in all scenarios, uses no water, and can last for almost 20 years without having to be refueled [61]. However, due to the operating pressure being 3.0 MPa on the primary side and 100 kPa on the secondary side, this does not meet the intended design requirement of being able to operate at atmospheric pressure.

2.2.8 eVinci Micro Reactor (Westinghouse)

The eVinci reactor is a TRISO fueled reactor that utilizes Heat pipes to convey the heat away from the core and to the heat conversion system. The fuel in the eVinci is enriched between 5 and 19.75 wt%. The thermal and electrical capacity are 7-12 MWt and 2-3.5 MWe, respectively. The eVinci is not pressurized and requires refuelling on a 36-month cycle. The major advantages of the eVinci include [61, p. 299]:

1. It will be manufactured and fueled in a factory and then transported to an end user site.

2. Heat is removed passively via the use of heat pipes which reduces the number

moving parts and making the overall design simpler.

Despite the advantages that come from heat pipes, they aren't without their disadvantages. Heat pipes do make the design simpler, but using them in a reactor core is a new heat transfer approach, and there is still significant analysis, testing, and qualification to be performed on their safety case in reactor cores. Additional disadvantages of heat pipe technology are captured in Section 2.1.4.

2.2.9 Aurora (Oklo)

The Aurora reactor is a 4 MWt and 1.5 MWe metallic uranium-zirconium fueled fast reactor. The Aurora uses supercritical CO_2 for its power conversion system [61, p. 297-298]. The major advantages of the Aurora reactor include:

1. It has a power output that is within the exact range that would be applicable for a remote Canadian community.
2. It is not pressurized.
3. Can last up to 20 years without having to be refuelled.
4. Small enough to be easily deployed to any community across Canada.

Other than the disadvantages of heat pipes outlined in Section 2.1.4, the other disadvantage of the Aurora reactor is that it is a fast reactor, which Canada does not have much experience with. Additional disadvantages around fast reactors are outlined in Section 2.1.1.

2.2.10 SSTAR and SUPERSTAR

The lead cooled reactor that is used as a reference design for Generation IV reactors is the Small Secure Transportable Autonomous Reactor (SSTAR), which is a fast reactor utilizing trans-uranium (TRU) nitride metallic fuel and uses natural

convection of the lead for cooling during both operational and shutdown heat removal [28]. It utilizes a supercritical CO_2 Brayton cycle and can operate from 15 to 30 years. It also has the major advantage that it is completely sealed and designed for complete modular replacement, meaning it would never be refuelled onsite, and the entire reactor would be replaced as a "cassette" [28, p. 137]. The advantages of the SSTAR system include the fact that it was intended to be used for remote locations, it is easily transportable on ship or truck, it requires no refuelling for large spans of time, and it can provide upwards of 20 MWe of power [66]. A pre-conceptual schematic is shown in Figure 2.19.

The SSTAR reactor has now been superseded by the latest iteration of the design, which is now called the Sustainable Proliferation-resistance Enhanced Refined Secure Transportable Autonomous Reactor (SUPERSTAR). SUPERSTAR is a 300 MWt/120 MWe reactor that is a liquid lead natural convection cooled fast reactor. Its fuel is particulate-based U-Pu-Zr metallic fuel with weapons grade Plutonium that is <12 wt%. The SUPERSTAR includes all of the advantages of the SSTAR core; however, it has a larger thermal and electrical capacity, as well as higher inlet and outlet temperatures, 400°C and 480°C, respectively [61, p. 237-240]. The reactor power is much larger than what is actually needed for a remote Canadian community, and it utilizes plutonium in its fuel which will more than likely cause challenges with local communities and the Canadian Nuclear Safety Commission.

2.2.11 SEALER (LeadCold)

LeadCold SEALER Reactor is a 3 MWe lead cooled fast reactor that is enriched with 19.75% to 19.9% UO_2 fuel. It was designed to meet the demands for commercial power production in Arctic Canadian regions such as Nunavut and the North-West Territories. A schematic of SEALER is shown in Figure 2.20. The

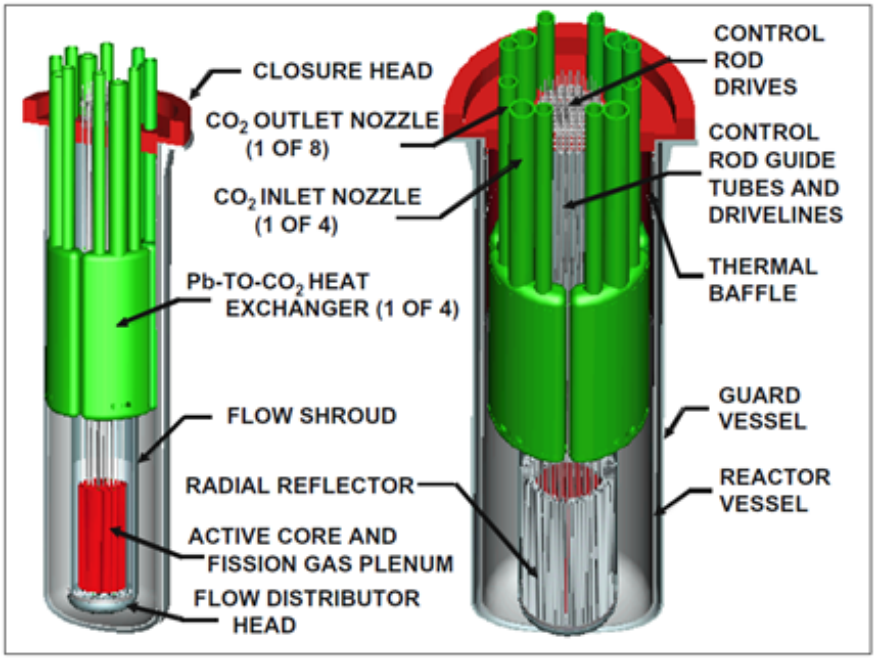

Figure 2.19: Pre-conceptual schematic of SSTAR [28, p. 139].

SEALER can operate for 27 full power years when operating at 8 MWth. The average coolant temperature at the outlet is kept below 430°C, and results in a maximum cladding temperature below 450°C. Unlike the SSTAR design, the SEALER utilizes forced convection to maintain appropriate core cooling [67].

The major advantages of the SEALER core include:

1. It was specifically designed for Arctic communities in Canada.
2. Operates at atmospheric pressure.
3. Is easily transportable.
4. Can power the average Arctic community.

The major disadvantage is that it utilizes a fast neutron spectrum, which may make it difficult to control and go through the licensing process in Canada.

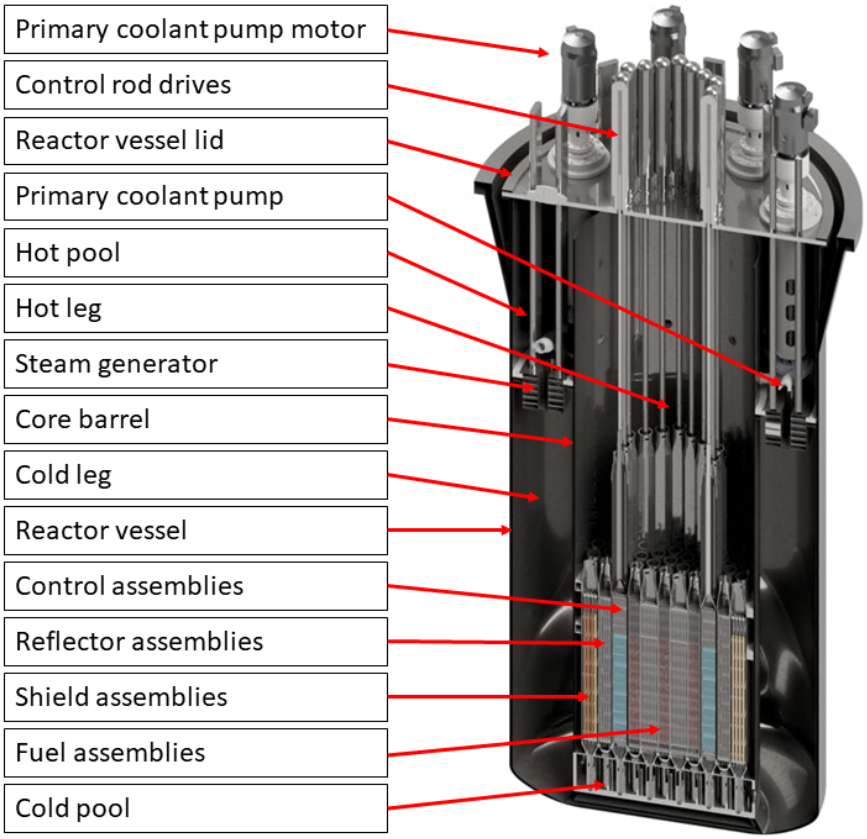

Figure 2.20: Schematic of LeadCold's SEALER design. Taken from [67].

Chapter 3

The ZAN4e Reactor

All reactor systems reviewed in the previous chapter possess some desirable features that make them potentially useful in remote arctic communities. However, none of them meet all the requirements in Table 1.1. This chapter presents a novel microreactor design developed specifically for use in remote Canadian arctic communities, one which attempts to satisfy almost all criteria in Table 1.1.

3.1 Main Design Features and Core Parameters

The ZAN4e (**Z**ero-degree **A**rctic **N**atural-circulation **4** MW **e**lectric) thermal reactor is unpressurized, lead cooled, graphite moderated, and uses High-Assay Low-Enriched (HALEU) fuel. Stirling engines heated directly by the primary-circuit lead coolant are used to convert heat to work and drive the electrical generators without needing a water-based turbine secondary circuit. In addition, coolant circulation is achieved by natural convection without the use of pumps.

Using graphite as a moderator avoids possible core damage resulting from the volume increase of water when freezing [68], an essential consideration for the arctic climate. The lead coolant can withstand high temperatures without boiling (boiling point is 1737°C) leading to improved efficiency of the Stirling

engines and, compared to sodium and water, is comparatively benign and does not support chemical interactions that can lead to energy release in the event of accident conditions [28]. As an added advantage, lead does not expand when solidifying, thus avoiding potential mechanical damage to the core if the reactor has to be shut down in the absence of external power, a probable scenario in an off-grid arctic location.

The ZAN4e core consists of a 1.7 m-tall vertical graphite cylinder pierced axially by 13 vertical cylindrical fuel channels, which consist of two concentric tubes separated by a gas gap for thermal insulation. The inner tubes contain the fuel assemblies and natural lead coolant. Fuel channels are arranged in a rectangular array with a pitch of 28.575 cm. The overall reactor diagram is shown in Figure 3.1.

The graphite moderator is sealed in a stainless-steel vessel in order to avoid contact with air and consequent oxidation. Even in the event of an air-ingress accident (i.e., oxygen entering the reactor core as well as the stainless-steel vessel), the graphite blocks will oxidize and lose mass, but the unique atomic crystal structure of nuclear grade graphite will prevent self-sustained burning [69].

The core is located at the bottom of an inner stainless-steel reactor vessel, which is cylindrical in shape, taller than the core, and with a hemispherical bottom. The inner reactor vessel has transfer holes both at the bottom and at the top. The hole diameter (20.7 cm), is twice the diameter of the inner fuel channel tube diameter, which is large enough to present only minimal resistance to coolant circulation. The inner vessel is contained in the outer reactor vessel, which is a cylinder with a larger radius than the inner vessel. The difference in radii is sufficient to accommodate 13 Stirling-engine cylinders arranged in a circular array at the top of the two vessels and to present minimal hydraulic resistance to the convection flow of coolant.

The cooler lead enters the core at the bottom, is heated up in the fuel channels, reaches the plenum at the top of the core, then exits the inner vessel through the top transfer holes, whereby it heats up the Stirling-engine cylinders. Having transferred heat to the Stirling-engine cylinders, the cooler lead moves downwards through the downcomer between the two vessels and re-enters the inner vessel through the bottom transfer holes, reaching the bottom of the core again.

The fuel assemblies have CANDU-like-geometry (i.e., 37-element annular cluster), thus relying on well-established technology, and use HALEU fuel to provide sufficient reactivity for the small core and to ensure a sufficient period of time between refueling. A longitudinal cross-section through the fuel channels and core is shown in Figure 3.1, Figure 3.2 shows an axial cross-section through the core, and Figure 3.3 shows an axial cross-section through the core at the Stirling Engine level. All three figures are to scale.

There are several heat-to-electricity conversion methodologies and techniques that could have been used. However, the microreactor design for the Canadian arctic employed the use of Stirling engines for a few important reasons. First, its primary coolant used in the Stirling engine is a gas which will not freeze in the event of a reactor shutdown, spurious trip, or malfunction. Second, their size is much smaller than typical turbine generator sets and can more easily be incorporated into an integrated modular unit with the reactor. Third, a Stirling Engine is highly efficient when used in high-temperature environments and with the use of an ideal gas such as helium or hydrogen [70]. The major downfall of Stirling Engines is that it is still unclear the total lifetime that they can achieve [70]. However, due to the use of CANDU style geometry enriched UO_2 fuel, the time till a refuel is required is less than three years (to be confirmed later in the thesis). Stirling Engines have been shown to have a continuous operating capability of 5,000 to 10,000 hours, which will require 1, maybe 2, short periods

of shutdown to perform maintenance on the Stirling Engines [71].

Determining the thermal output of the reactor is based on the power needs of remote communities in Canada. Based on the Remote Communities Energy Database (RCED), 86.2% of remote communities currently have a total fossil fuel generation capacity that is less than or equal to 3.5 MWe, as shown in Figure 1.2. The goal of the ZAN4e is to replace the generating capacity of already existing infrastructure in these remote communities. Considering that 86.2% of communities already have a generating capacity in the range of 3.5 MWe, it was decided that the ZAN4e would cover the higher end of this range and produce at most 3.5 MWe.

A goal of the ZAN4e reactor is to have the capability to provide district heating. As a result, the temperature of the heat sink for the Stirling engines was chosen to be 75°C to account for heat losses from the reactor core to the surrounding homes of Arctic communities [72, p. 3, 111, 115, 116]. The outlet temperature of the reactor core was chosen to be 900°C. This temperature is largely based on the thermal shock limitation (i.e., the largest temperature change that an object can survive before it begins to fail) on the zircaloy cladding of the fuel. With an inlet temperature of 400℃, the zircaloy will start to experience thermal shock when outlet temperatures are >900℃ [73]. With the efficiency of the Stirling engines, the required thermal output of the reactor core could then be determined using Eq. 3.1 by solving for E_F. For those communities that require less electrical capacity (i.e., <3.5 MWe), more district or process heat can be provided to these communities as an alternative opportunity to handle the extra generating capacity of the reactor.

There are several systems and subsystems that need to be designed when replacing diesel power generation with a nuclear microreactor. For example, the Stirling Engines, reactor vessel, containment/confinement structure, shielding,

reactivity control system, etc. However, the focus of this research, as it relates to the design of a microreactor for a remote Canadian community, is on the reactor core, meaning it focuses on the neutronics and thermal-hydraulics of the core. All other things are not explained or discussed in detail as these will be further developed in later design stages of the ZAN4e.

The main core and fuel-channel parameters are shown in Table 3.1.

Table 3.1: ZAN4e Parameters

Core Parameter	**Value**	**Core Parameter**	**Value**
Effective core diameter w/o reflector	1.46 m	Inner tube, inner radius	5.169 cm
Core diameter with graphite reflector	2.0 m	Inner tube, outer radius	5.603 cm
Core height	1.7 m	Outer tube, inner radius	6.448 cm
Fuel channel pitch	28.575 cm	Outer tube, outer radius	6.588 cm
Inlet Temperature	400℃	1st Ring Radius	1.489 cm
Outlet temperature	900℃	2nd Ring Radius	2.876 cm
Total core thermal power	10 MW_th	3rd Ring Radius	4.331 cm

Continued on next page

Table 3.1: ZAN4e Parameters (Continued)

Core Parameter	Value	Core Parameter	Value
Graphite temperature	400℃	Fuel pellet radius	0.608 cm
Maximum Fuel Centerline temperature	2050℃	Fuel element radius (fuel + Zircaloy4)	6.540 cm
Molten lead average coolant temperature	650℃	Core Life	2.75 yr
Molted Lead Core Mass Flow Rate	140 kg/s	Lead Boiling Point	1740℃

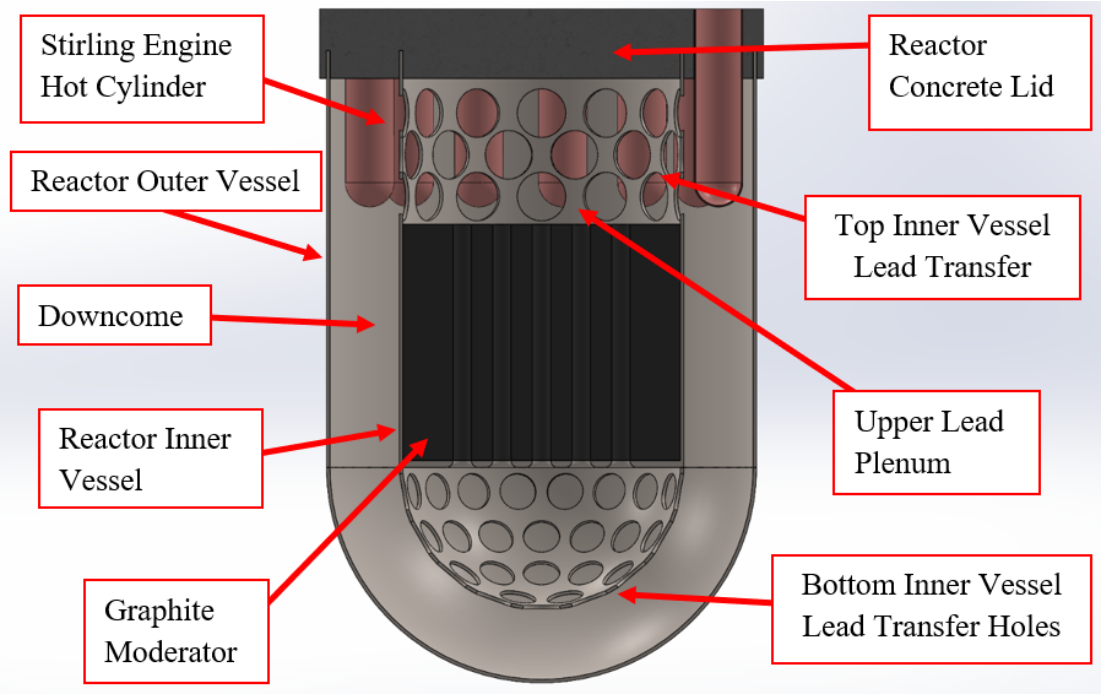

Figure 3.1: ZAN4e Reactor Diagram: longitudinal cross-section.

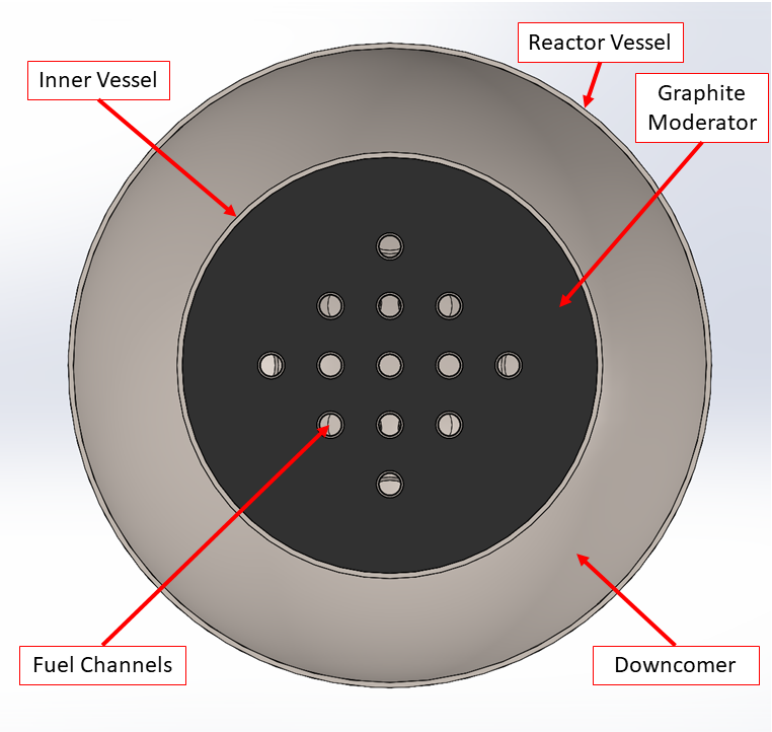

Figure 3.2: ZAN4e Reactor Diagram: axial cross-section at the fuel level.

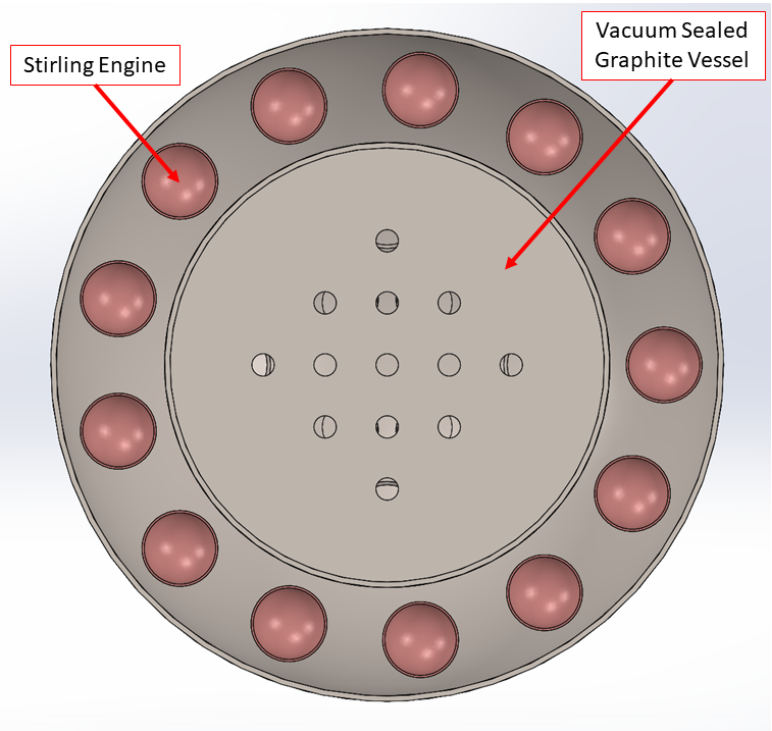

Figure 3.3: ZAN4e Reactor Diagram: axial cross-section at the Stirling-engine level.

3.2 Core Analysis

The core performance is analyzed from a neutronics and thermal-hydraulic perspective to demonstrate that the design is feasible and that safety limits are not exceeded. Neutronics calculations are performed using the lattice transport code DRAGON [74] and the core diffusion code DONJON [75]. The thermal-hydraulic analysis is performed using well-accepted correlations. The use of Serpent, a continuous-energy Monte Carlo reactor physics burnup calculation code, was also used as a tool for scoping calculations and to confirm the results obtained from DRAGON and DONJON.

Upon determining the power output of the ZAN4e, the iterative design and analysis process for the ZAN4e went as follows [76, p. 505-506], and is depicted in 3.4:

- Determine the maximum acceptable linear power density in the hottest channel, taking into account both steady-state and transient operating conditions.
- Determine the appropriate fuel-to-moderator ratio by choosing a lattice pitch length.
- Choose initial fuel enrichment.
- Perform a burnup calculation to find the core life and determine how long criticality can be maintained.
- Determine the various hot channel factors characterizing the core, using both computer codes describing the core neutronics and thermal-hydraulic behaviour.
- Calculate the bulk coolant and fuel centerline temperatures.

- Determine core diameter.

The iterative design methodology shown in 3.4 was followed until the centerline fuel temperature had sufficient margin from its melting point. Considering that the melting point of UO_2 is 2850℃ an approximate 30% margin was selected which means that to determine a final core geometry the centerline fuel temperature needs to be no more than 2050℃.

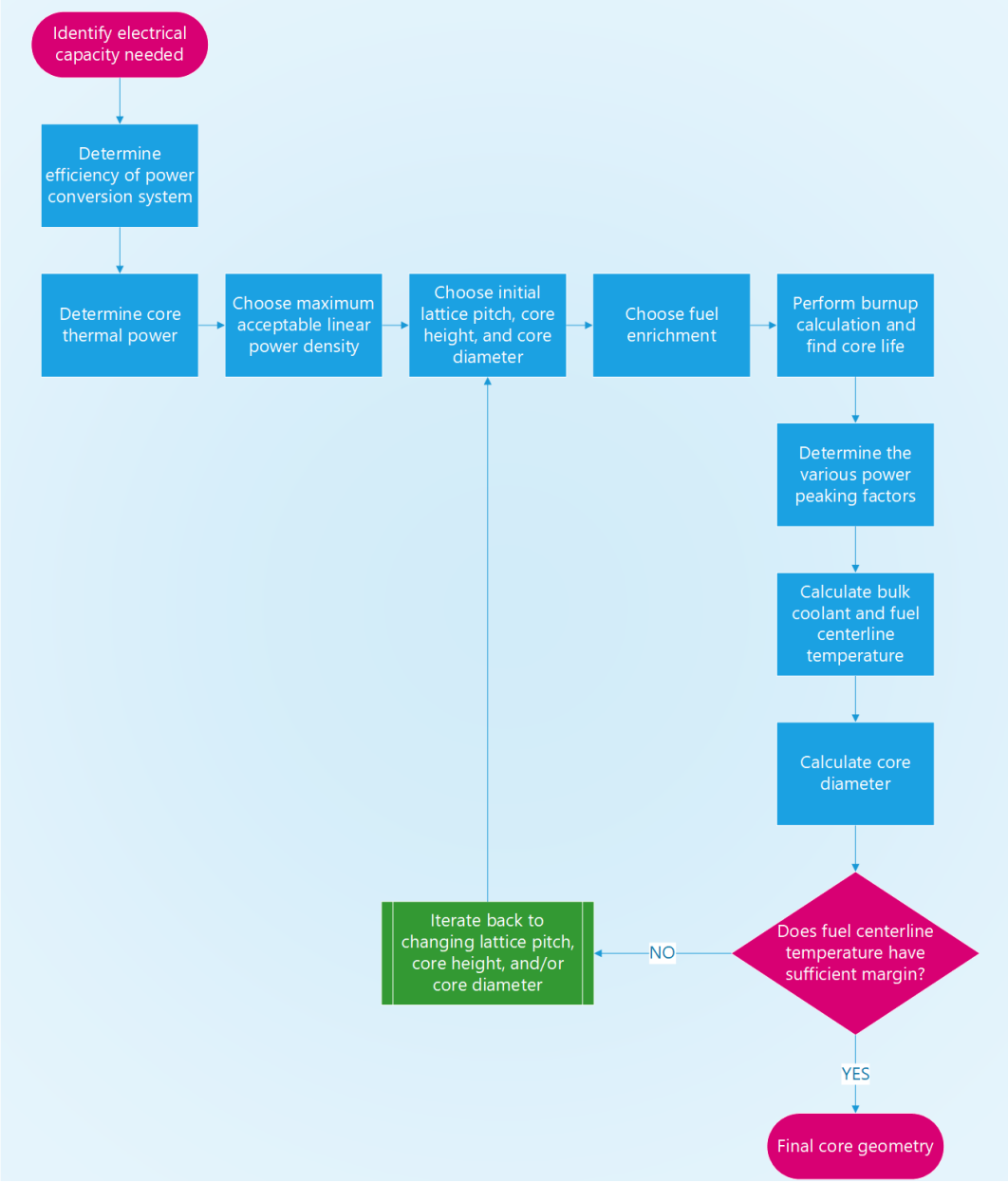

Figure 3.4: Iterative design methodology followed for ZAN4e.

3.2.1 Overall Plant Energy Balance

To determine the size of the reactor core, it was necessary to first determine the thermal output required by the reactor core based on the efficiency of the Stirling engines.

As mentioned in the previous section, the required electrical capacity that a microreactor should have for a remote community in Canada is approximately 3.5 MWe. Using this requirement, along with the approximate net overall thermal efficiency of the Stirling engines, the thermal power used in the ZAN4e reactor can be evaluated using Eq. 3.1 [36, p. 98-99].

$$\eta = \frac{P_{net}}{E_F} = \left(1 - \frac{T_C}{T_H}\right) \cdot C \cdot \eta_H \cdot \eta_M \cdot f_A \tag{3.1}$$

In Eq. 3.1, η_{eff} is the overall thermal efficiency, P_{net} is the net shaft power, and E_F is the total energy flow, which equals the thermal power from the reactor (Wth). C is the Carnot efficiency ratio of Stirling-engine efficiency to Carnot efficiency (normally from 0.65 to 0.75), η_H is the heater efficiency which is the ratio between the energy flow to the heater and the total energy flow (typically 0.90), η_M is the mechanical efficiency (typically 0.90), and f_A is the auxiliary ratio (typically 0.95) [36, p. 98-99]. Assuming the hot-cylinder temperature, T_H, to be equal to the average coolant temperature of 650°C and the cold-cylinder temperature T_C, to be equal to 75°C (necessary to drive the district-heating system, [72]), the Stirling-engine efficiency is found to be 35%. Ignoring losses, the available electrical power can be estimated to be 3.5 MW, and the district-heating power can be estimated to be 6.5 MW, assuming a thermal power output of the reactor to be 10 MWth.

The type of Stirling Engine design that will be employed in the microreactor will be either a beta-type or gamma-type Stirling Engine, as shown in Figure 2.8.

In the Stirling Engine analysis, the use of the Schmidt Cycle was used to get

an initial estimation of the size and performance to be used with the microreactor. A Schmidt cycle Stirling engine is one where the power piston and displacer, or the two power pistons, move sinusoidally with each other. In using the Schmidt Analysis, there are several assumptions that are made, which include [36, p. 71]:

1. Sinusoidal motion of parts.
2. Known and constant gas temperatures in all parts of the engine.
3. No gas leakage.
4. Working fluid obeys perfect gas law.
5. At each instant in the cycle, the gas pressure is the same through the working gas.

When utilizing a diameter of 15 cm, a height of 50 cm, 3.5 moles of helium gas inventory, a hot gas temperature of 650℃, and a cold gas temperature of 75℃, the Stirling engine is able to produce approximately 350 kWe, assuming a cycle frequency of 60 Hz. With 13 Stirling engines all operating at 350 kWe, you get a total electrical capacity of approximately 4.5 MWe, which is more than what is needed for the ZAN4e. However, the potential for uprating the electrical capacity to >3.5 MWe exists.

The variables that govern Stirling Engines, as shown above, can be manipulated in various ways to arrive at a solution that will produce a Stirling Engine that produces upwards of 350 kWe. For example, the quantity of gas in the Stirling Engine can be increased, thus increasing the operating pressure, which would in turn increase the power output. If the pressure is increased, then the radius and/or height of the Stirling Engine can be reduced to get the same amount of power. To ensure feasibility in the design of the Stirling Engine, it is important to ensure that the size is not too large. As a result, it is proposed to consider

the use of Heat Pipes extending down from the bottom of the Stirling Engines to support accurate and reliable heat removal from the core as is done in heat pipe Stirling Engine nuclear reactors used for space applications [77].

3.2.2 Neutronic Analysis

The aims of the neutronic analysis are four-fold:

1. Determine the core reactivity as a function of the lattice pitch.
2. Determine the fuel burnup as a function of fuel enrichment.
3. Determine the power-peaking factors.
4. Determine the core life.

Neutronics calculations are performed in two steps: a lattice-calculation step and a core calculation step. Lattice calculations are performed in two dimensions for a lattice cell consisting of a fuel channel and associated moderator. They produce cell-averaged burnup-dependent two-group macroscopic cross sections to be used in the core calculation. All lattice calculations employ the collision-probabilities method and are performed using the lattice code DRAGON [74] and the WIMS-D Library Update 69-group microscopic cross-section library [78]. The lattice cell geometry used in DRAGON is shown in Figure 3.5. In Figure 3.5 there are additional "rings" within the same material cell (same colour) that allow for increased simulation accuracy by splitting the geometry into n radial meshes to support simulation. All cell-boundary conditions are reflective. Core-level calculations use a cell-homogenized reactor model. They employ the finite-difference method in two-group diffusion theory in a Cartesian geometry and are performed using the code DONJON [75]. The geometrical model utilized in DONJON is shown in Figure 3.7. The number of meshes is $90 \times 90 \times 50$ in the

x, y, and z directions, respectively. Vacuum boundary conditions are imposed on all external core boundaries.

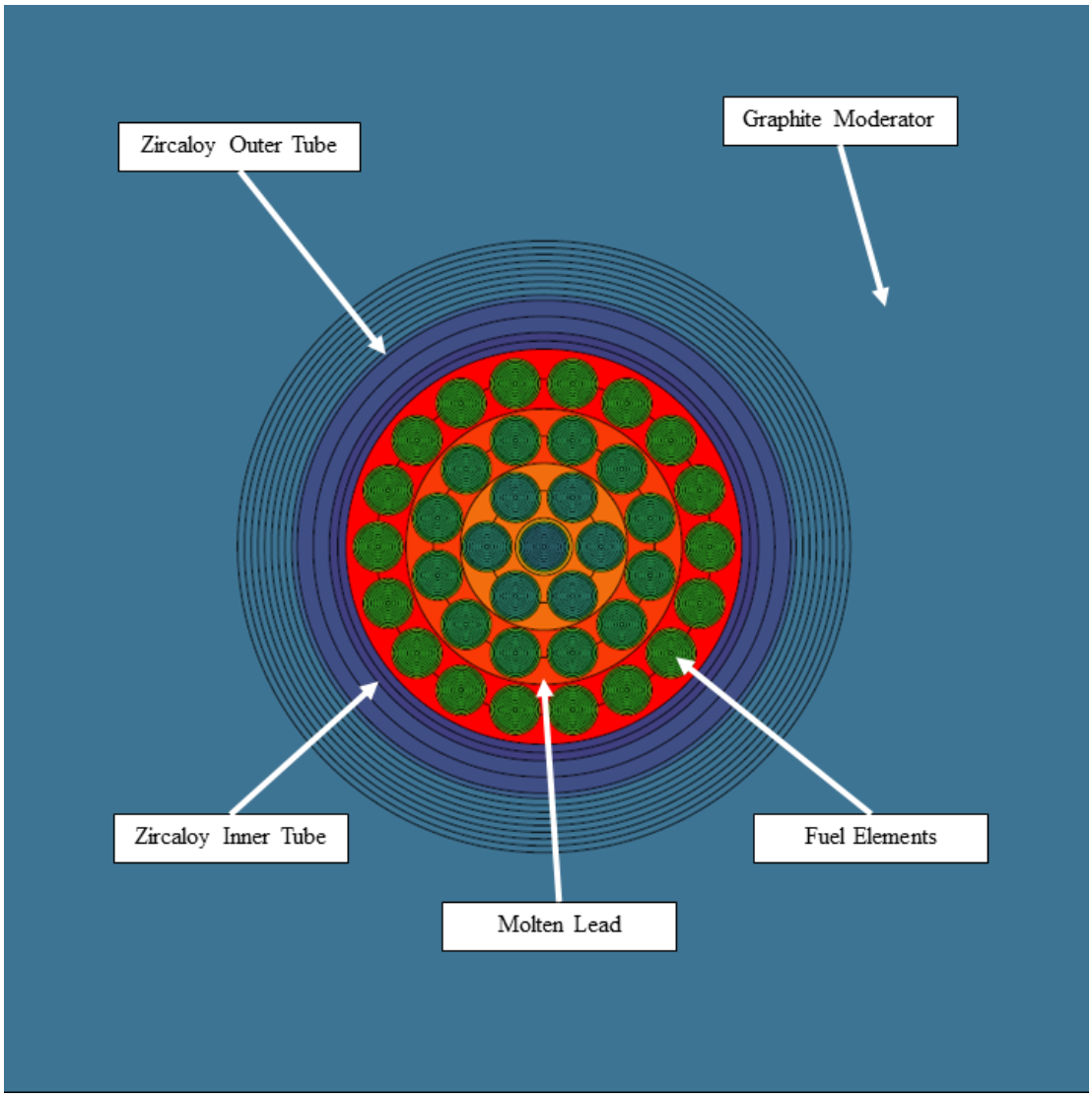

Figure 3.5: Lattice cell geometry used in DRAGON

The methodology that was followed is derived from [79] and is shown in Figure 3.6. The nuclear data in ENDF/B was processed into a 69-group microscopic cross-section library using NJOY. The conversion of ENDF/B to an isotopic cross-section library via NJOY was outside the scope of this thesis. Rather, the WLUP 69-group microscopic cross-section library [78] was used directly in lattice calculations.

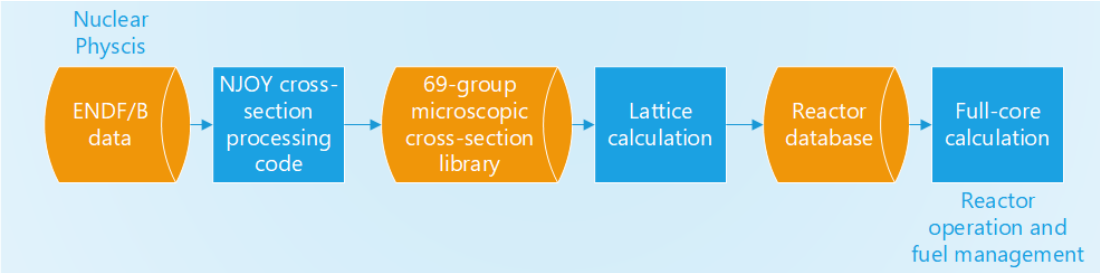

Figure 3.6: Data for to go from nuclear physics data to a full-core calculation [79, p. 54]

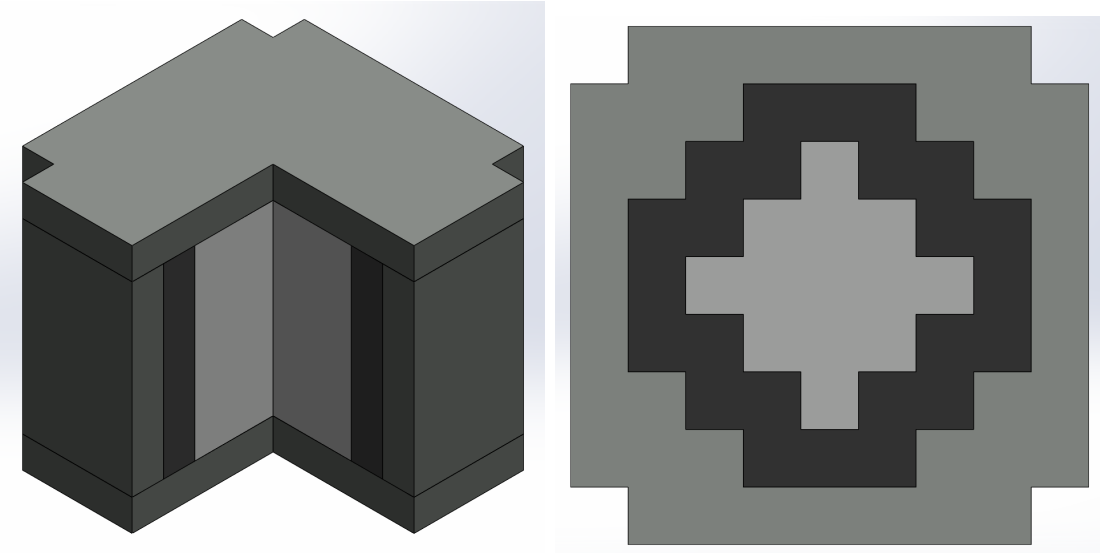

(a) Isometric view (b) cross-sectional view

Figure 3.7: DONJON model views. Homogenized fuel cells are shown in light grey. Lead cells are shown in intermediate grey. Graphite cells are shown in dark grey.

The lattice calculation allowed for a small database to be built of the burnup-dependent two-group macroscopic lattice-homogenized cross sections. This lattice cell consisted of a single fuel bundle (i.e., 37 elements) surrounded by a pressure tube, thermal gas gap, outer support tube, and graphite moderator [79, p. 195]. This lattice cell is typically simulated without any knowledge of the operating conditions of the reactor. The macroscopic cross sections that are calculated via the lattice calculation are later used as inputs for the full core calculation, as outlined in Figure 3.6.

With the thermal output of the reactor core determined, the size of the core was then able to be determined using Eg. 3.2 [76, p. 506]. However, before Eq. 3.2 can be fully solved, the values for the pitch, p, the linear power density, q'_{MAX}, the hot channel factor, F_q^N, and the height of the core, H, need to be determined.

$$D_{core} = \left[\frac{4p^2 MW_{th} F_q^N}{\pi q'_{MAX} H} \right] \tag{3.2}$$

To arrive at a value for the diameter of the core, a few of the variables in Eq. 3.2 needed to be iteratively adjusted. As outlined in [76, p. 479], it outlines that the linear power density of the fuel needs to be kept below a maximum linear power density of 660 W/cm, otherwise, the uranium fuel will begin to melt. Most power reactors keep their maximum linear power density in the operating range of 420-460 W/cm [76, p. 479]. As a result, the core was analyzed with an initial maximum linear power density of 450 W/cm. The height of the core was chosen such that it would ensure the maximum linear power density did not exceed 450 W/cm.

Lattice Pitch

The lattice pitch affects the core reactivity, its size, weight and, consequently, transportability.

The dependence of the fresh-core effective multiplication factor on the lattice pitch is shown in Figure 3.8. Results shown in Figure 3.8 indicate that the fresh-core multiplication factor increases up to a pitch of 38 cm. However, to limit the size and overall weight of the core, a 28.575 cm pitch, identical to that of the CANDU reactor, is used. As can be seen from Figure 3.8, the use of a 28.575 cm pitch only results in an approximately 400 pcm penalty in the core reactivity.

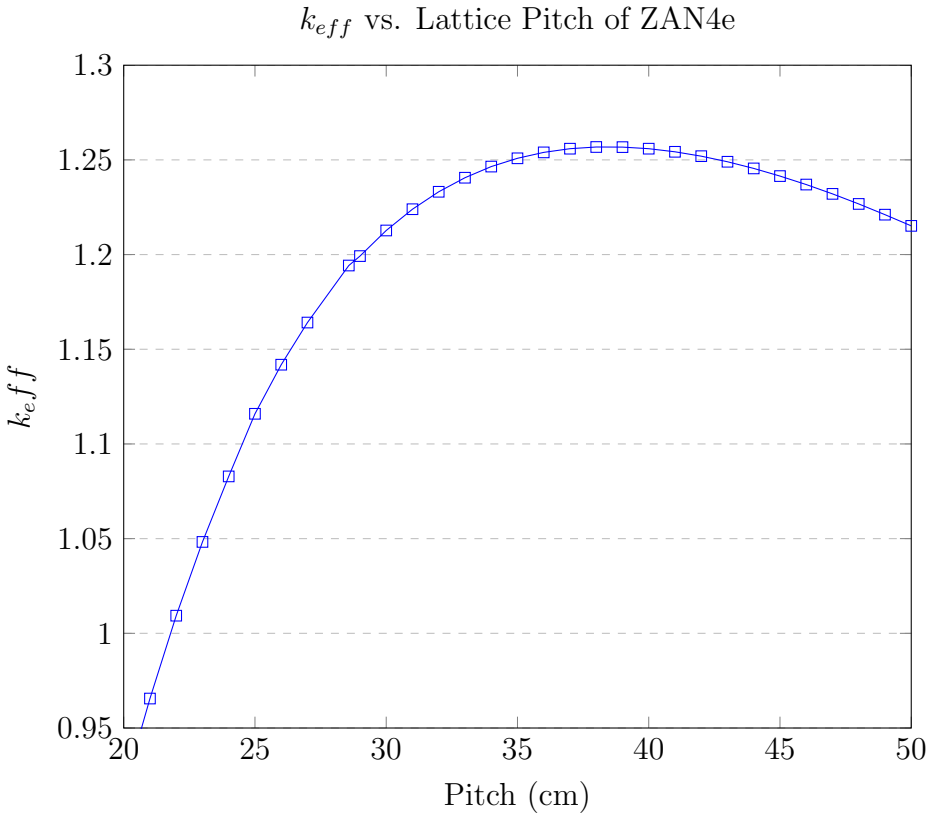

Figure 3.8: Core effective multiplication factor vs. lattice pitch for the ZAN4e reactor

Enrichment and Fuel Burnup

CANDU-type fuel assemblies have been shown to operate safely up to a burnup of 21 MWd/kgU [80]. Therefore, the core is assumed not to exceed a maximum assembly burnup of 20 MWd/kgU.

Figure 3.9 shows the relationship between the core reactivity and the maximum assembly burnup for different levels of enrichment. Core reactivity is found from a full-core two-group diffusion calculation.

Curves in Figure 3.9 include a 7000 pcm reduction in reactivity to account for additional absorbers in the core that are not explicitly modelled, such as structural materials. The value used is based on that for a 660 MWe PHWR core [81] and is adjusted for the smaller size of the ZAN4e core. It is likely an overestimate of what the real reactivity decrease due to additional absorbers will be. As can be seen from Figure 3.9, a 10% fuel enrichment is the enrichment value chosen for the ZAN4e and is sufficient to ensure core criticality just past 20 MWd/kgU.

Power Peaking Factors

The flux results of the DONJON simulation were normalized to the total thermal power of the ZAN4e (i.e., 10 MWth) to find the thermal power in each fuel channel. In DONJON, each fuel channel was split into 50 "bins" or calculational regions. The flux values obtained from DONJON were per lattice cell (i.e., 1 to 13) and per bin (i.e., 1 to 50). As a result, when normalizing the flux values to the total reactor thermal power the result that was obtained was the total thermal power produced in each bin of each fuel channel. The unnormalized power for each bin in each fuel channel was calculated according to Equation 3.3.

$$P_{i,j} = \Big((\phi_{i,j}\Sigma_{i,j})_{fast} + (\phi_{i,j}\Sigma_{i,j})_{thermal} \Big) E_{fiss} V_{bin} \tag{3.3}$$

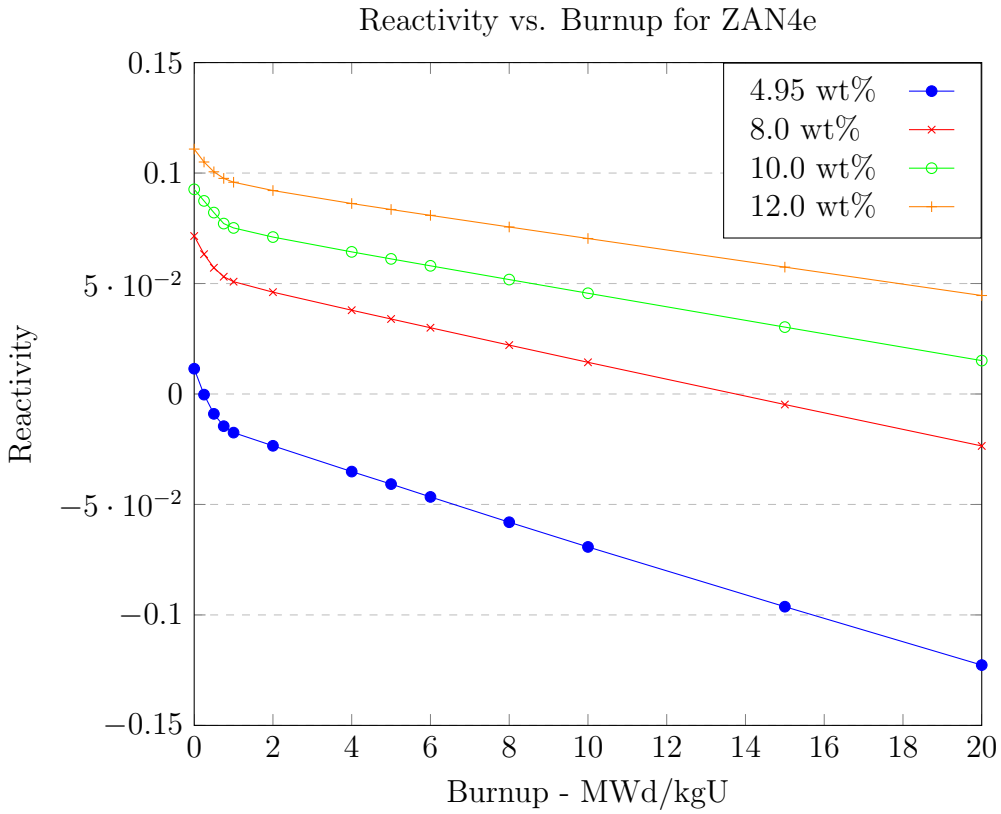

Figure 3.9: Core reactivity as a function of maximum burnup for various levels of enrichment

Where $P_{i,j}$ represents the unnormalized power matrix in each bin (i) of each fuel channel (j), $(\phi_{i,j}\Sigma_{i,j})_{fast}$ is the fast flux and macroscopic fission cross-section at a given fuel channel and bin, $(\phi_{i,j}\Sigma_{i,j})_{thermal}$ is the thermal flux and macroscopic fission cross-section at a given fuel channel and bin, E_{fiss} is the energy produced per fission, V_{bin} is the volume of each bin.

The normalizing factor is then able to be found by dividing the total thermal power of the ZAN4e by the summation of the unnoramlized power in each fuel channel and bin, as shown in 3.4.

$$\alpha_{norm} = \frac{P_{thermal}}{\sum_{i=1}^{13}\sum_{j=1}^{50}\Big((\phi_{i,j}\Sigma_{i,j})_{fast} + (\phi_{i,j}\Sigma_{i,j})_{thermal}\Big)E_{fiss}V_{bin}} \tag{3.4}$$

Using the normalizing factor, α_{norm}, the power produced in each bin of each

fuel channel is then able to be calculated using 3.5.

$$P_{i,j}^{norm} = \alpha_{norm} P_{i,j} \tag{3.5}$$

Where $P_{i,j}^{norm}$ is the normalized power matrix for the ZAN4e which represents the actual thermal power produced in each of the 50 bins per fuel channel. The linear power density q' in each bin of each fuel channel is then able to be calculated by taking the power produced in the given bin and dividing it by the height of the bin.

The radial power peaking factor, F_R, is calculated using Eq. 3.6 [76].

$$F_R = \frac{\int_{-H/2}^{H/2} q'_{HC}(z)\, dz}{\frac{1}{13}\sum_{i=1}^{13} \int_{-H/2}^{H/2} q'_i(z)\, dz} = \frac{q_{HC}}{\frac{1}{13}\sum_{i=1}^{13} q_i} \tag{3.6}$$

In Eq. 3.6, $q'(z)$ represents the linear channel power, q represents the channel power. The HC subscript denotes the hot channel (channel with maximum power), and i is a generic channel index.

The axial power peaking factor, F_Z, is calculated using Eq. 3.7 [76].

$$F_Z = \frac{max_z q'_{HC}(z)}{\frac{1}{H}\int_{-H/2}^{H/2} q'_{HC}(z)\, dz} \tag{3.7}$$

The numerator of Eq. 3.7 represents the maximum linear power of the hot channel, and the denominator represents the average linear power of the hot channel. Finally, the pin power-peaking factor, F_P, is determined as the ratio between the maximum linear pin power density and the average linear pin power density for a fuel assembly, both taken at the same axial position, as expressed by Eq. 3.8.

$$F_p = \frac{q'_{k-max}(z)}{\frac{1}{37}\sum_{k=1}^{37} q'_i(z)} \tag{3.8}$$

Within a fuel assembly, the thermal flux, and hence the pin power, increases with the distance between the pin centre and the centre of the bundle. This is illustrated schematically in Figure 3.10, reproduced from [82]. Consequently, the hot pin is found in the outer ring.

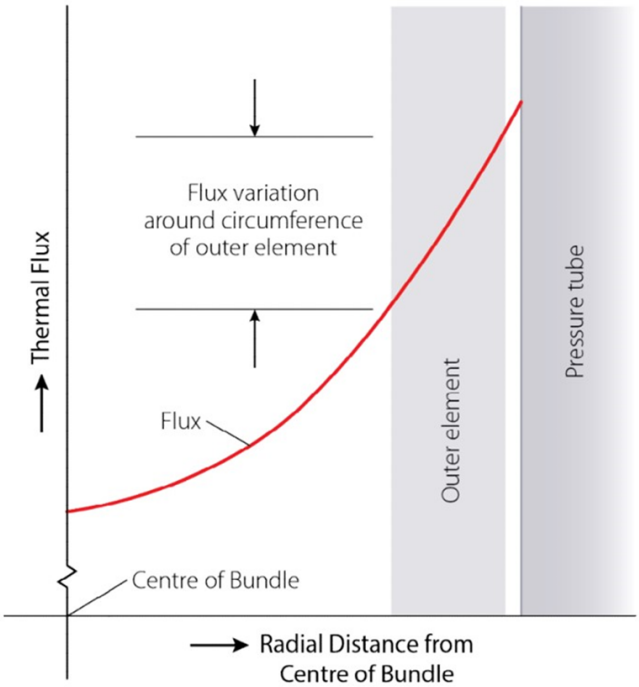

Figure 3.10: Illustrative circumferential variation in flux of thermal neutrons (reproduced from [82])

The linear power for pin k, q', is determined using the one-group flux, ϕ_k, the one-group fission cross-section, Σ_{fk}, the Energy per fission, E_{fk}, and the pin cross-section area A_p, and is calculated using Eq. 3.9.

$$q'_k = \phi_k \Sigma_{fk} E_f A_p \tag{3.9}$$

Eq. 3.8 and 3.9 can be combined into,

$$F_p = \frac{\phi_{k-max} \Sigma_{fk-max} E_f A_p}{\frac{\sum_{k=1}^{37} \phi_k \Sigma_{fk} E_f A_p}{37}} \tag{3.10}$$

The overall power-peaking factor of the ZAN4e is simply found by finding the

product of the radial power-peaking factor, axial power-peaking factor, and pin power-peaking factor, as shown in Eq. 3.11.

$$F_q^N = F_R F_Z F_p \tag{3.11}$$

Table 3.2 summarizes all of the power-peaking factors calculated for the ZAN4e using DRAGON and DONJON.

Table 3.2: Power peaking factors for the ZAN4e

F_R	F_Z	F_p	F_q
1.22	1.36	1.42	2.34

The overall power peaking factor of the ZAN4e core is smaller than the 3.64 power peaking factor for a theoretical homogenous, bare cylindrical core [76, p. 503]. This is due to the neutron-reflecting properties of the graphite and lead surrounding the core both laterally and at the top and bottom. The power peaking factor of the ZAN4e is also competitive with a typical zone-loaded PWR, which is 2.6 [76, p. 503].

Based on the core parameters, the mass of all the major ZAN4e components are shown in Table 3.3.

Table 3.3: Mass of ZAN4e Components

ZAN4e Component	**Mass (kg)**
Moderator	11,288
Inner Vessel	4,947
Outer Vessel	8,796

Continued on next page

Table 3.3: Mass of ZAN4e Components (Continued)

ZAN4e Component	**Mass (kg)**
Lid	9,947
Fuel	1,004
Lead Coolant	227,667
Total	263,651

Core Life

The maximum allowable assembly burnup ($B_{max} = 20MWd/kg$), together with the core thermal power ($P_{th} = 10MW$), the mass of core fuel, m_{fuel}, and axial and radial power peaking factors, $F_{RZ} = F_R \cdot F_Z$, determine the core life. Using Eq. 3.12, the core life is found to be 2.75 years. The experiments performed at the Bruce were based on the burnup of the bundle, hence why only the radial and axial peaking factors were used to estimate the core life [80].

$$T_{core} = \frac{B_{max} \frac{1}{F_{RZ}} m_{fuel}}{P_{th}} \tag{3.12}$$

As it relates to refuelling after 2.75 years, the burned ZAN4e core will be transported back to a commercial warehouse facility, where it will be decommissioned and sent to the appropriate spent fuel storage location, which is yet to be determined. A new ZAN4e modular unit will then replace the one that has been fully burned. The large quantity of lead inside the reactor will provide significant shielding for transport.

3.2.3 Thermal-hydraulic Analysis

In calculating a lot of the thermal-hydraulic parameters, an important parameter that needs to be calculated is the heat-transfer coefficient for molten lead. There are two correlations for the Nusselt number that are typically used for liquid metal coolants for flow in circular tubes.

Lead Parameters

For constant heat flux along the tube wall (Lyon-Martinelli):

$$Nu = 7 + 0.025Pe^{0.8} \tag{3.13}$$

For uniform wall temperature (Seban and Shimazaki):

$$Nu = 5.0 + 0.025Pe^{0.8} \tag{3.14}$$

An important note to make is that, as shown in the Peclet number, the viscosity is eliminated, which reflects the fact that viscosity is not the rate-determining parameter in liquid-metal heat transfer [33, p. 268].

There are three other correlations that have been used when estimating the Nusselt number for different conditions. The Kazimi and Carelli correlation was one of the first correlations that was used for Liquid Metal Fast Breeder Reactors (LMFBRs). The correlation is,

$$Nu = 4.0 + 0.16R^5 + 0.33R^{3.8}(0.01Pe)^{0.86} \tag{3.15}$$

The Kazimi and Carelli correlation can be used when the Peclet number is less than 5,000 and the P/D (pitch to diameter) ratio (R=P/D) is between 1.1 and 1.4 [83, p. 832].The only downfall of the Kazimi and Carelli correlation is that

it underestimates the Nusselt number when P/D is high and is more for square lattice fuel assemblies. The other two correlations that have been used previously by Westinghouse include the Schad correlation and the Borishanskii correlation, as shown in Eq. 3.16, 3.17, 3.18, and 3.19.

Schad Correlation:

$$Nu = 4.5[-16.5 + ... + 24.96R - 8.55R^2] \quad (for Pe \leq 150) \tag{3.16}$$

$$Nu = [-16.5 + ... + 24.96R - 8.55R^2]Pe^{0.3} \quad (for 150 < Pe < 150) \tag{3.17}$$

Borishanskii Correlation:

$$Nu = 24.15log[-8.12 + 12.76R - 3.65R^2] \quad (for Pe < 200) \tag{3.18}$$

$$\begin{aligned} Nu = 24.15log[-8.12 + 12.76R - 3.65R^2] + \\ 0.0175[1 - e^{6(1-R)}](Pe - 200)^{0.9} \quad (for 200 \leq Pe \leq 2,000) \end{aligned} \tag{3.19}$$

Using Eq. 3.13, the average heat transfer coefficient was calculated to be 23,365.1 W/m^2K.

Lead Parameters

The lead parameters that were used for the ZAN4e were based on the equations, data, and values published by the Nuclear Energy Agency (NEA) in the 2015 Edition of *Handbook on Lead-bismuth Eutectic Alloy and Lead Properties, Materials Compatibility, Thermal-hydraulics and Technologies* [30]. The Handbook on Lead-bismuth Eutectic Alloy and Lead Properties, Materials Compatibility, Thermal-hydraulics and Technologies contained several equations that could be used to determine the given value of a parameter as a function of temperature.

The parameters that were investigated for lead included its density, dynamic viscosity, heat capacity, thermal conductivity, volume expansion, and kinematic viscosity. The equations that were used for each of these parameters are shown below, where T in each of the equations represents the temperature of the molten lead.

Density of lead (kg/m^3):

$$\rho = 11,441 - 1.2795T \tag{3.20}$$

Dynamic viscosity of lead ($Pa \cdot s$):

$$\mu = (4.55 \times 10^{-4}) exp\left(\frac{1069}{T}\right) \tag{3.21}$$

Heat capacity of lead (J/kgK):

$$c_p = 175.1 - (4.961 \cdot 10^{-2})T + (1.985 \cdot 10^{-5})T^2 - (2.099 \cdot 10^{-9})T^3 - (1.524 \cdot 10^{6})T^{-2} \tag{3.22}$$

Volume expansion of lead ($1/K$):

$$\gamma = \frac{1}{8942 - T} \tag{3.23}$$

Kinematic Viscosity of lead:

$$\nu = \frac{\mu}{\rho} \tag{3.24}$$

Coolant Mass Flow Rate

The necessary mass flow rate in any channel, i, is determined using Eq. 3.25, using the channel power, q_i, determined from a DONJON full-core diffusion calculation,

and the inlet and outlet temperatures of the coolant.

$$\dot{m}_i = \frac{q_i}{c_p(T_o - T_i)} \tag{3.25}$$

It is assumed that the coolant flow rate through each channel is adjusted (e.g., using diaphragms) so that the inlet and outlet temperatures are the same for all channels, as shown in Figure 3.11.

		8.94		
	10.99	11.81	10.99	
8.94	11.81	13.11	11.81	8.94
	10.99	11.81	10.99	
		8.94		

Figure 3.11: Mass flow rate map (kg/s)

The necessary total coolant mass flow rate through the core is determined by summing the mass flow rates through all 13 channels of the core:

$$\dot{m}_{tot} = \frac{P_{th}}{c_p(T_o - T_i)} \tag{3.26}$$

The value of the total coolant mass flow rate is found to be 140.08 kg/s.

Axial Coolant Temperature and Fuel Temperature Profiles

The bulk coolant temperature is found numerically in 50 axial bins, using Eq. 3.27.

$$T_n^{fl} = T_{n-1}^{fl} + \sum_{j=1}^{n} \frac{q'(z_{j-1})\Delta z_j}{\dot{m} c_p(T_{j-1}^{fl})} \tag{3.27}$$

where n represents the bin of interest, and q' represents the channel linear power density.

The centreline fuel temperature is determined using Eq. 3.28 [76, p. 482].

$$T_{CL}(z) = T^{fl}(z) + \frac{q'(z)}{2\pi r_F}\left[\frac{r_F}{2\bar{k}_F} + \frac{1}{h_G} + \frac{t_C}{k_C} + \frac{r_F}{h_s(r_F + t_C}\right] \tag{3.28}$$

The centerline and bulk coolant temperatures for each channel of the core are calculated for a fresh core and an end-of-life core. The axial power profiles for the pin of maximum power are shown in Figure 3.12, for both the actual core and a bare (no graphite reflector and no surrounding lead coolant) core. The corresponding fuel centerline temperature profiles for a fresh core and an end-of-life core are shown in Figure 3.13 and Figure 3.14, respectively.

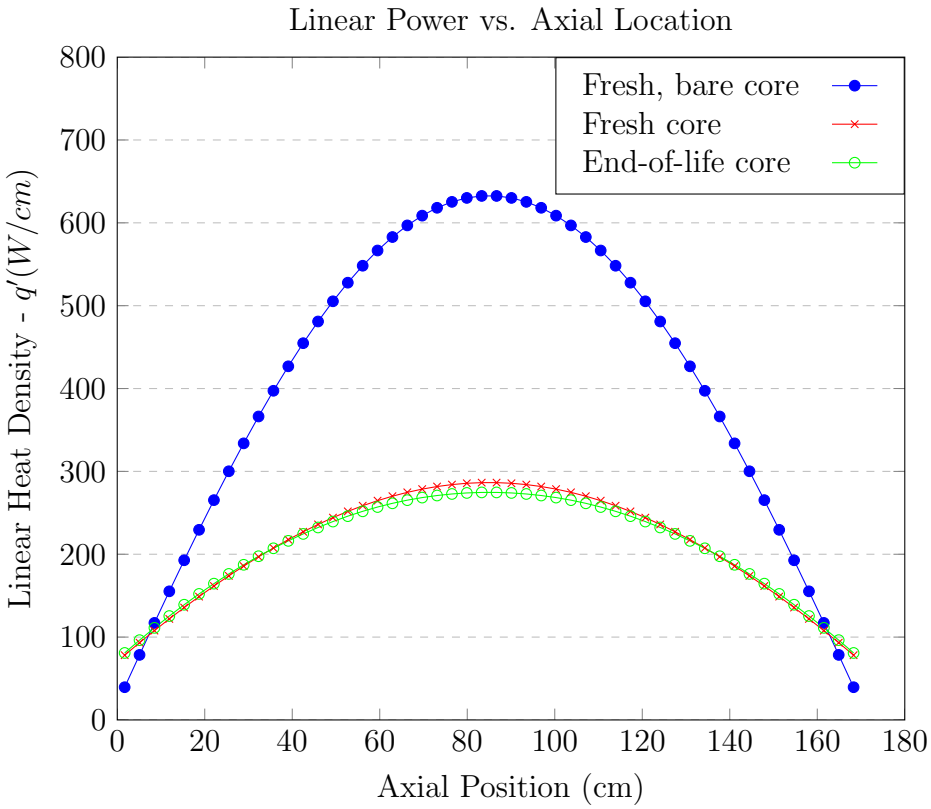

Figure 3.12: Linear power density of outer pin for a fresh bare core, fresh normal core, and a normal end-of-life core.

Figure 3.12 illustrates the point that the low axial power-peaking factor of the ZAN4e core is due to the presence of reflector graphite and lead. It also shows

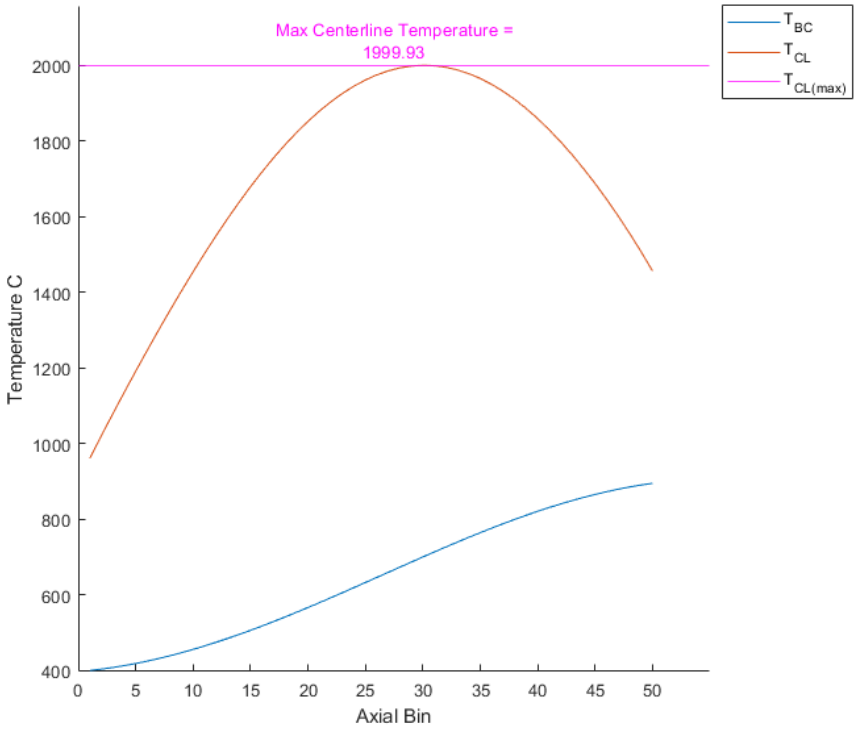

Figure 3.13: Centreline (orange) and Bulk Coolant (blue) temperature profiles for a fresh core.

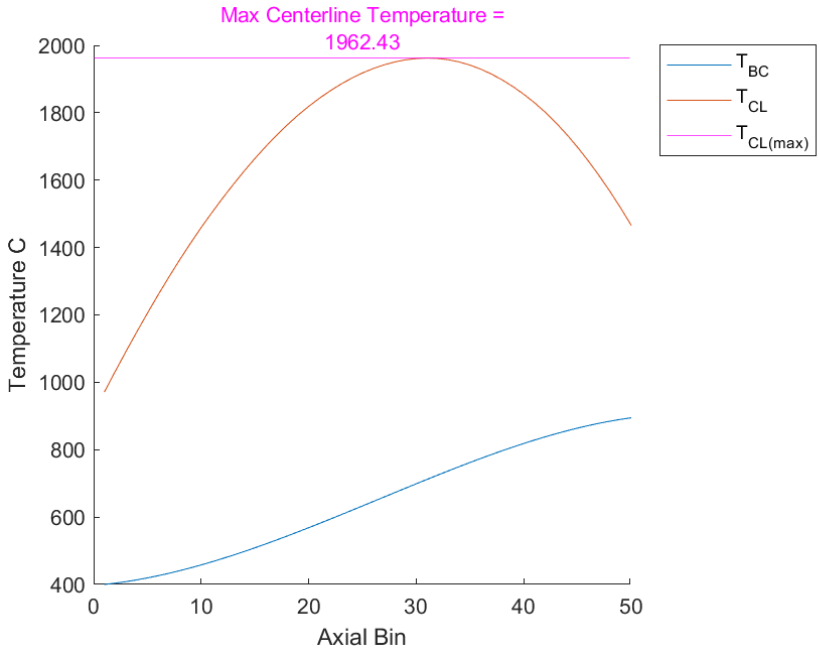

Figure 3.14: Centreline (orange) and Bulk Coolant (blue) temperature profiles for an end-of-life core.

that the end-of-life core has a slightly flatter axial power profile due to the higher burnup of the fuel located closer to the midplane of the reactor.

Figure 3.13 and Figure 3.14 confirm that the calculated coolant mass flow rates result in the desired channel outlet temperature of 900°C. They also show that the maximum fuel centerline temperature for a fresh and end-of-life core are 1999.93°C and 1962.43°C, respectively. Thus, the fuel is expected to remain well below the 2850°C melting point during normal operation.

Coolant Circulation Through Natural Convection

An important safety feature of the ZAN4e reactor is its ability to use natural convection for coolant circulation. The physics that allows for natural convection of the lead coolant to occur is the difference in densities of the lead between the high and low-temperature locations of the reactor. Eq. 3.29 expresses the static pressure available to circulate the coolant through thermo-syphon, and forms the foundation of the preliminary natural convection model outlined in this section.

$$\Delta P_{static} = (\rho_L - \rho_{avg}) g L_{core} + (\rho_L - \rho_H) g L_{abovecore} \tag{3.29}$$

Where ΔP_{static} is the static pressure available to push the lead coolant in the core, ρ_{avg} is the average density in the reactor core, ρ_L is the density of lead at the lowest temperature in the reactor (i.e., 400°C), ρ_H is the density at the highest temperature in the reactor (i.e., 900°C), g is the gravitational acceleration (i.e., 9.81 m/s2), L_{core} is the height of the core (i.e., 1.7 m), and $L_{abovecore}$ is the height between the top of the core and the bottom of the Stirling engines.

For natural convection to occur in the core, the friction pressure losses in the core need to be less than the available static pressure in the core. The friction pressure loss across a tube with an arbitrary-shape cross section is calculated

using Eq. 3.30, where f is the Fanning friction factor.

$$\Delta P = 2\left(\frac{L}{D_{hydraulic}}\right)\rho\bar{u}_z^2 f \tag{3.30}$$

Using the necessary mass flow rate, the flow velocity is calculated using Eq. 3.31.

$$\bar{u}_z = \frac{\dot{m}}{\rho A} \tag{3.31}$$

The Reynolds number is found using Eq. 3.32.

$$Re = \frac{\rho\bar{u}_z D_{hydraulic}}{\mu} \tag{3.32}$$

In Eq. 3.32, μ is the dynamic viscosity of lead in Pa, and $D_{hydraulic}$ is the hydraulic diameter, found according to [76]:

$$D_{hydraulic} = \frac{4S}{Z} \tag{3.33}$$

Where S is the flow area, and Z is the wetted perimeter of the flow.

The hydraulic diameter depends on the size and shape of the tube cross-section. For this analysis, five different hydraulic diameters were used, corresponding to a core channel, region above the core, region around each Stirling engine, the downcomer, and region below the core. It will be noted that the pressure drop across one channel is representative of the pressure drop across the core.

Values of the Reynolds number are found to exceed 2,100 in all five regions. Consequently, the flow in all five regions is found to be turbulent and, hence, the Fanning friction factor, f, is found using Blasius' formula [76, p. 485]:

$$f = 0.0791 Re^{-0.25} \tag{3.34}$$

The lead density and dynamic viscosity are calculated based on Eq. 3.20 and 3.21.

The pressure loss due to the lead coolant making 180° turns at the top and bottom of the reactor is estimated using Eq. 3.35 [84, p. 433-440].

$$\Delta p = K_L \frac{1}{2} \rho \bar{u}_z^2 \tag{3.35}$$

where K_L is the loss coefficient based on the flow geometry, ρ is the density of the fluid, and $\bar{u}_z$ is the average velocity of the fluid. The loss coefficient for a 180° turn is 0.2. Pressure losses through the transfer holes are estimated by using the formula for the pressure loss induced by an orifice plate in a pipe, as shown by Eq. 3.36 [84, p. 460-462].

$$\Delta P = \frac{1}{2} \rho (1 - \beta^4) \left(\frac{\dot{m}}{\rho C_o A_o} \right)^2 = (1 - \beta^4) \frac{1}{C_o^2} \frac{1}{2} \rho \bar{u}_z^2 \tag{3.36}$$

In Eq. 3.36, ρ is the density of the fluid, $\dot{m}$ is the mass flow rate through the orifice, A_o is the area of the orifice opening, C_o is the orifice discharge coefficient, β is the ratio of the orifice diameter to the pipe diameter, and $\bar{u}_z$ is the average fluid velocity through the orifice. The discharge coefficient decreases slightly as the Reynolds number in the full pipe increases and also decreases slightly as β decreases, reaching a minimum of 0.6 for $Re = \infty$ and $\beta = 0$ [84]. The maximum theoretical pressure loss corresponds to the minimum value of the discharge coefficient, namely $C_o = 0.6$, and to the maximum value of the coefficient $(1 - \beta^4)$, namely 1. It is this maximum theoretical pressure drop, shown in Eq. 3.37, that is used in this work to estimate the pressure drop through the transfer holes.

$$\Delta P = \frac{1}{0.6^2} \frac{1}{2} \rho \bar{u}_z^2 \tag{3.37}$$

The parameters used in determining the static driving pressure and the friction pressure losses are shown in Table 3.4.

Table 3.4: Parameters and values used in analysis

	900°C	**400°C**	**650°C**
$\rho_{Pb}(T)[kg/m^3]$	9,939.95	10,579.70	10,259.8
$\mu_{Pb}[Pa \cdot s]$	1.132E-03	2.227E-03	1.680E-03
Other Important Parameters			
$d_{element}$	1.308 cm	L_{core}	1.70 m
$d_{stirling}$	0.35 m	$L_{stirling}$	0.5 m
		$L_{abovecore}$	1.425 m
		$L_{reactor}$	3.125 m

The static pressure is found to be $\Delta P_{static} = 19,769Pa$, and the determined friction pressure losses are shown in Table 3.5. Values in Table 3.5 include an additional 25% margin over values calculated using Eq. 3.35, 3.36, and 3.37.

Table 3.5: Pressure losses in ZAN4e

	$D_h[m]$	$\dot{m}[kg/s]$	$u_z[m/s]$	Re	$\Delta P_f[Pa]$
Above the Core	2.0	140.1	0.00449	78,794	0.0022
Stirling Engines	0.34	140.1	0.0085	25,214	0.0010
Downcomer	1	140.1	0.0033	15,786	0.0066
Below the Core	1	140.1	0.0033	15,786	0.0028
Core (center channel)	0.0074	14.5	0.41418	21,761	5,253.6
180 turn (top)		140.1	0.0085		0.0898

Continued on next page

Table 3.5: Pressure losses in ZAN4e (Continued)

	$D_h[m]$	$\dot{m}[kg/s]$	$u_z[m/s]$	Re	$\Delta P_f[Pa]$
180 turn (bottom)		140.1	0.0033		0.0144
Transfer holes (top and bottom)	0.21	3.6	0.0104		3.853
Total					5,257.6

Table 3.5 shows that pressure losses are dominated by the pressure loss in the fuel channels, which accounts for more than 99% of the total pressure loss. Consequently, even though the pressure losses for regions of complex geometry, such as the Stirling Engine region and the transfer holes, are estimated using relatively coarse approximations, recalculating them using detailed models is not expected to yield substantial changes in the overall result. As a result, because the total pressure loss in Table 3.5 (5,257.6 Pa) is much smaller than the static pressure driving the flow (19,769 Pa), the condition for natural circulation is theoretically satisfied with a large margin.

3.2.4 Other Design Considerations

Start-up Methodology

There are two main approaches that could be taken regarding how the lead can be melted. First, the fuel and coolant could be shipped separately from the reactor. This would ultimately guarantee a sub-critical state, reduce the transport weight, and allow for the molten lead to be melted outside of the core in a controlled process and then pumped into the core when appropriate. This process adds extra steps in reactor start-up via assembly and the need for additional equipment on-site to handle the lead, heat it up, and pump it into the core. This option

is unfeasible in terms of what happens after the reactor shuts down and then needs to be started back up again, as the lead will be solidified and then needs to somehow be removed from the core and melted again.

The second, simpler option is to have electrical heaters directly in the core to melt the lead for start-up, both for the first core and after shut-down states. There could be guide tubes in the core that would allow for heaters to vertically penetrate the outer plenum and above the core to provide heat to the solidified lead. Another option is to have a slightly thicker inner vessel that would have small spaced penetrations to allow for electric heaters to be inserted and supply heat to the solidified lead. Diesel generators would still be needed, however, they would be focused on providing direct electrical power to the heaters.

Ultimately, a more detailed analysis needs to be performed in thermal analysis and CFD to arrive at an appropriate solution.

Reactivity Control Methodology

The conceptual design for the reactivity control system will mainly leverage the use of control and shutdown rods vertically penetrating the core, more than likely through holes drilled in the moderator and inserted guide tubes. Further kinetics analyses need to be performed to determine the negative reactivity supplied from the temperature coefficients of the fuel and moderator and how that may be leveraged as a control strategy in addition to control rods.

HALEU Fuel Supply Chain

Hight Assay Low Enriched Uranium (HALEU) is currently a risk for many advanced reactor companies. The U.S. Department of Energy (DOE) understands this risk and is working to provide funding and resources to develop American enrichment capabilities and a domestic HALEU supply chain [85], [86]. One of the

leading suppliers in the U.S. is Centrus Energy, which is working with domestic partners to increase HALEU availability [87].

Corrosion, Erosion, and Material Selection

In a high-temperature lead environment, the consequences of corrosion and erosion can be reduced by the selection of the right materials. There are three main interfaces in the reactor core with the molten lead: graphite, steel reactor vessel, and zircaloy fuel bundles.

Several experiments have been performed that have shown that nuclear-grade graphite is highly resistant to corrosion and erosion when placed in a high-temperature molten lead environment. When various grades of commercial nuclear graphite were placed in 800°C molten lead, under a range of pressures, it was observed that the ultrafine-grained graphite had the best barrier properties due to its incredibly small pore size [88]. Ultrafine-grained nuclear graphite is also highly corrosion resistant at elevated temperatures of 800°C. One of the main solutions to avoid corrosion of steel in the high-temperature lead environment is the use of surface coatings. One of the main surface coatings that has some of the best results in terms of its corrosion resistance is Al-containing coatings [89]. Aluminum based coatings also maintain their structural integrity upon "irradiation, thermal cycling, cyclic nano impact and scratch" [90].

Some testing has been performed, showing that zirconium CANDU geometry bundles have good compatibility with molten lead. Testing was done by immersing a CANDU bundle into the molten lead at 420℃. The results showed that there was no sign of corrosion [91, p. 111-112]. Further testing will need to be performed to account for increased lead temperatures in the ZAN4e, as well as to analyze how it operates under various transient and operating conditions.

The conclusions of this analysis are based on the assumption that the materials

utilized in the reactor can withstand large temperature gradients. For example, the Stirling Engine is currently designed to handle an average temperature of 650°C on the hot side and 75°C on the cold side. A future Material selection analysis may indicate that the use of such exotic materials to reach the large temperature gradients stipulated in the design is not feasible.

Chapter 4

Conclusions and Future Work

The conceptual design of the ZAN4e has shown the initial feasibility to further design work for future applications in the Canadian arctic. The graphite moderated, lead-cooled, enriched reactor is capable of running for 2.75 years before refuelling needs to occur and can maintain cooling purely through natural convection. The two main objectives of this research were to:

1. Develop a conceptual design for a microreactor that is adequate for remote Canadian Arctic communities.

2. Demonstrate that the proposed microreactor design satisfies basic functional and safety requirements.

Section 3 meets the first objective by showing the development of a conceptual design of a microreactor for remote Canadian Arctic communities. The second objective is met via the requirements traceability matrix, as shown in Table 4.1, which identifies where each design requirement is incorporated into the design of the ZAN4e.

Table 4.1: Requirements traceability matrix for ZAN4e.

ID	Requirement	Design Compliance
F1	Shall be able to offer electricity as well as central heating for arctic communities.	Section 3.2.1 outlines the use of Stirling engines for power conversion and the minimum capacity it will have for the ZAN4e.
F2	All structures, systems, and components of the reactor shall be enclosed in a single containment structure that can be transported as one unit.	Figure 3.1 shows ZAN4e has Stirling engines built in as an integral unit.
P1	Shall have an electrical output of approximately 3.5 MWe, corresponding to the power capacity needs of the majority of arctic communities.	Section 3.2.1 outlines the minimum electrical capacity for the ZAN4e.

Continued on next page

Table 4.1: Requirements traceability matrix for ZAN4e. (Continued)

ID	Requirement	Design Compliance
P2	Shall be transportable by ship, train, plane, or truck.	Based on the dimensions and weight of the ZAN4e, it should have no major issues being transported by the CC-177 Globemaster III transport plan, and as such it should be able to be transported by ship, train, and truck. However, a more detailed study needs to be performed on the available ship, train, and truck options that could transport the ZAN4e.
P3	Shall not exceed 72,500 kg.	Table 3.3 shows that without lead coolant the ZAN4e is less than 72,500 kg.
P4	Shall have dimensions less than 26.82 m (88 ft) in length and 3.76 m (12.33 ft) in diameter.	Table 3.1 shows that the height and diameter are less than 26.82 m and 3.76 m, respectively.
P5	Shall be able to last at least two years without having to be refueled.	Section 3.2.2 outlines core life of ZAN4e.

Continued on next page

Table 4.1: Requirements traceability matrix for ZAN4e. (Continued)

ID	Requirement	Design Compliance
P6	Reactor shall maintain structural integrity in temperatures as low as -75°C.	A thermal and structural analysis needs to be performed on the ZAN4e to show large temperature swings in cold climates. Section 3.1 outlines that the coolant and moderator will not cause expansion and structural integrity issues at low temperatures.
P7	Coolant shall not expand when freezing.	Section 3.1 outlines that the graphite moderator and lead coolant do not expand when freezing.
P8	Shall have fuel enrichment less than 20 wt% U-235 to avoid difficulties with sourcing enriched fuel.	Section 3.2.2 states that the level of enrichment for the ZAN4e is 10 wt%.
S1	Coolant shall not have a volatile reaction with wator or air.	Section 2.1.3 and 3.1 outline that the lead coolant is benign to water and air.
S2	Shall operate at atmospheric pressure.	Section 3.2.3 indicates that the core is cooled via natural circulation and as a result no pressurization is required.
S3	Shall employ natural convection cooling in the core.	Section 3.2.3 indicates that the core is cooled via natural circulation.

Continued on next page

Table 4.1: Requirements traceability matrix for ZAN4e. (Continued)

ID	Requirement	Design Compliance
E1	Shall be able to be removed from the operation site without any permanent damage to the local environment.	A set-up and construction methodology still needs to be determined to ensure that this requirement is satisfied.

The major next steps that need to be taken include a more detailed analysis of the natural convection cooling aspect of the ZAN4e. Only hand calculations have been performed showing its potential capability, but Computational Fluid Dynamic (CFD) and flow analyses, using CFD software, need to be performed to verify that the ZAN4e is capable of maintaining natural convection cooling throughout its life and under various modes and states.

Reactor dynamics and kinetics analyses needs to be performed to determine how the ZAN4e operates over time and under various operating conditions. All of the reactivity coefficients also need to be calculated in unison with the dynamics analyses. Negative reactivity for control also needs to be analyzed. Research will be performed in the future to see if the use of a SiC layer between the graphite blocks and stain-less steel vessel will reduce the effects of accident scenarios for air-ingress accidents [69]. Future studies will also be conducted to determine the most optimal hole diameter and spacing at the top and bottom of the inner vessel.

To potentially improve neutron economy, an analysis will be performed to investigate the use of 100% Pb-208 as the isotope of choice for the molten coolant, considering that the Pb-208 lead isotope has a lower neutron absorption cross-section compared to that of natural lead [31]. An adequate microscopic cross-section library that includes Pb-208 will have to be used for those calculations. To better increase the fuel utilization in the core and flatten the flux, investigating

zone loading the core (i.e., using different fuel enrichments in different locations) as well as possible alternative fuel arrangements will be investigated.

Bibliography

[1] Natural Resources Canada. "The atlas of canada - remote communities energy database." (2018), [Online]. Available: https://atlas.gc.ca/rced-bdece/en/index.html.

[2] Canada Energy Regulator. "Market snapshot: Overcoming the challenges of powering canada's off-grid communities." (2018), [Online]. Available: https://www.cer-rec.gc.ca/en/data-analysis/energy-markets/market-snapshots/2018/market-snapshot-overcoming-challenges-powering-canadas-off-grid-communities.html.

[3] Natural Resources Canada. "Status of remote/off-grid communities in canada." (2011), [Online]. Available: https://www.nrcan.gc.ca/sites/www.nrcan.gc.ca/files/canmetenergy/files/pubs/2013-118_en.pdf.

[4] K. DePippo and B. A. Peppley, "Canadian remote community power generation: How reformer and fuel cell systems compare with diesel generators," *International Journal of Energy Research*, vol. 43, no. 3, pp. 1161–1170, 2019.

[5] K. Force, "Presentation on the remote communities in canada and the remote communities energy database," Natural Resources Canada. [Online]. Available: https://www.irena.org/-/media/Files/IRENA/Agency/Events/2021/Feb/ORES-Slides/Day-3---Session-4.pdf?.

[6] Midcontinent Independent System Operator (MISO), "Transmission cost estimation guide for mtep22," Midcontinent Independent System Operator (MISO), Tech. Rep., Apr. 2022. [Online]. Available: https://cdn.misoenergy.org/Transmission%5C%20Cost%5C%20Estimation%5C%20Guide%5C%20for%5C%20MTEP22337433.pdf.

[7] Y. Touchette, P. Gass, and D. Echeverria, "Tracking diesel fuel subsidies in nunavut," WWF Canada, Tech. Rep., 2017. [Online]. Available: https://wwf.ca/wp-content/uploads/2020/03/Tracking-Diesel-Fuel-Subsidies_April-2017.pdf.

[8] Government of Canada. "Cc-177 globemaster procurement project." (2018), [Online]. Available: https://www.canada.ca/en/department-national-defence/services/procurement/cc-177-globemaster.html.

[9] U.S. Department of Energy, *DOE Fundamentals Handbook: Nuclear Physics and Reactor Theory*. U.S. Department of Energy, 1993, vol. 1 of 2.

[10] S. A. Alameri and A. K. Alkaabi, "Nuclear reactor technology development and utilization," in S. Ud-Din Khan and A. Nakhabov, Eds. Woodhead Publishing Series in Energy, 2020, ch. 1 - Fundamentals of Nuclear Reactors, pp. 27–60.

[11] International Atomic Energy Agency, "Status of fast reactor research and technology development," International Atomic Energy Agency, Tech. Rep. IAEA-TECDOC-1691, 2012. [Online]. Available: https://wwf.ca/wp-content/uploads/2020/03/Tracking-Diesel-Fuel-Subsidies_April-2017.pdf.

[12] N. Kasahara, *Fast Reactor System Design*. Springer Nature Singapore Pte Ltd., 2014.

[13] OECD Nuclear Energy Agency for the Generation IV International Forum, "Technology roadmap update for generation iv nuclear energy systems," OECD Nuclear Energy Agency for the Generation IV International Forum, Tech. Rep., 2014. [Online]. Available: https://www.gen-4.org/gif/jcms/c_60729/technology-roadmap-update-2013.

[14] J. R. Lamarsh and A. J. Baratta, *Introduction to Nuclear Engineering*, 4th. Pearson Education Inc., 2018.

[15] nuclear-power.com. "Cross-sections of uranium." (2022), [Online]. Available: https://www.nuclear-power.com/nuclear-power-plant/nuclear-fuel/uranium/cross-sections-of-uranium/.

[16] B. J. Lewis, E. N. Onder, and A. A. Prudil, *Fundamentals of Nuclear Engineering*, 1st. Wiley & Sons Ltd., 2017.

[17] J. J. Powers and B. D. Wirth, "A review of triso fuel performance models," *Journal of Nuclear Materials*, vol. 405, no. 1, 2010.

[18] Generation IV International Forum, "A technology roadmap for generation iv nuclear energy systems," U.S. DOE Nuclear Energy Research Advisory Committee, Tech. Rep. GIF-002-00, 2002. [Online]. Available: https://www.gen-4.org/gif/jcms/c_40473/a-technology-roadmap-for-generation-iv-nuclear-energy-systems.

[19] U.S. Nuclear Regulatory Commission - Office of Nuclear Regulatory Research, "Triso-coated particle fuel phenomenon identification and ranking tables (pirts) for fission product transport due to manufacturing, operations, and accidents," U.S. Nuclear Regulatory Commission, Tech. Rep. NUREG/CR-6844, Vol. 1, 2004.

[20] R. Moormann, "Fission product transport and source terms in htrs: Experience from avr pebble bed reactor," Institute of Energy Research, Tech. Rep., 2008. DOI: 10.1155/2008/597491.

[21] A. Sowder and C. Marciulescu, "Topical report on uranium oxycarbide (uco) tristructural isotropic (triso) coated particle fuel performance," in *NRC Topical Report Pre-submittal Meeting*, Electric Power Research Institute, Inc., 2019.

[22] M. Allibert, M. Aufiero, M. Brovchenko, *et al.*, "Handbook of generation iv nuclear reactors," in I. L. Pioro, Ed. Woodhead Publishing, 2016, ch. Molten salt fast reactors, pp. 157–188.

[23] D. LeBlanc, "Molten salt reactors: A new beginning for an old idea," *Nuclear Engineering and Design*, vol. 240, no. 6, pp. 1644–1656, 2010. DOI: 10.1016/j.nucengdes.2009.12.033.

[24] C. W. Forsberg, S. Lam, D. M. Carpenter, *et al.*, "Tritium control and capture in salt-cooled fission and fusion reactors: Status, challenges, and path forward," *Nuclear Technology*, vol. 197, no. 2, pp. 119–139, 2017. DOI: 10.13182/NT16-101.

[25] H. Cao, P. Sun, G. Luo, K. Wang, and X. Bai, "Lage-leak sodium-water reaction accident analysis of sodium-cooled fast reactor," *Progress in Nuclear Energy*, vol. 142, 2021. DOI: 10.1016/j.pnucene.2021.104010.

[26] V. Kriventsev and A. Yamaguchi, "Session 1: Sodium cooled fast smrs," in *Benefits and Challenges of Small Modular Fast Reactors*, International Atomic Energy Agency, 2021. [Online]. Available: https://www-pub.iaea.org/MTCD/Publications/PDF/TE-1972web.pdf.

[27] S. Kubo and H. Ohshima, "Handbook of generation iv nuclear reactors," in I. L. Pioro, Ed. Woodhead Publishing, 2016, ch. Sodium-cooled fast reactor, pp. 97–118.

[28] C. Smith and L. Cinotti, "Handbook of generation iv nuclear reactors," in I. L. Pioro, Ed. Woodhead Publishing, 2016, ch. Lead-cooled fast reactor, pp. 119–156.

[29] International Atomic Energy Agency, "Liquid metal cooled reactors: Experience in design and operation," International Atomic Energy Agency, Tech. Rep. IAEA-TECDOC-1569, 2007.

[30] Nuclear Energy Agency, *Handbook on Lead-bismuth Eutectic Alloy and Lead Properties, Material Compatibility, Thermal-hydraulics and Technologies*. Nuclear Energy Agency, Organisation for Economic Co-operation, and Development, 2015.

[31] G. L. Khorasanov and A. I. Blokhin, "Current research in nuclear reactor technology in brazil and worldwide," in A. Mesquita, Ed. IntechOpen, 2013, ch. 9 - Benefits in Using Lead-208 Coolant for Fast Reactors and Accelerator Driven Systems. DOI: 10.5772/56032.

[32] Generation IV International Forum, "A technology roadmap update for generation iv nuclear energy systems," OECD Nuclear Energy Agency, Tech. Rep., 2014.

[33] M. El-Wakil, *Nuclear Heat Transport*. The American Nuclear Society, 1981.

[34] A. N. Shmelev, G. G. Kulikov, V. A. Apse, E. G. Kulikov, and V. V. Artisyuk, "Radiogenic lead with dominant concent of 208pb: New coolant and neutron moderator for innovative nuclear facilities," *Science and Technology of Nuclear Installations*, vol. 2011, no. 2, 2011. DOI: 10.1155/2011/252903.

[35] L. S. Mason, "Comparison of energy conversion technologies for space nuclear power systems," National Aeronautics and Space Administration, Tech. Rep. NASA/TM-2019-219935, Dec. 2019.

[36] W. R. Martini, *Stirling Engine Design Manual*, Second. National Aeronautics and Space Administration, 1983.

[37] A. K. Almajri, S. Mahmoud, and R. Al-Dadah, "Modelling and parametric study of an efficient alpha type stirling engine," *Energy Conversion and Management*, vol. 145, no. 93, 2017.

[38] W. Uchman, L. Remiorz, K. Grzywnowicz, and J. Kotowicz, "Parametric analysis of a beta stirling engine – a prime mover for distributed," *Applied Thermal Engineering*, vol. 145, no. 693, 2018.

[39] A. Abuelyamen and R. Ben-Mansour, "Energy efficiency comparison of stirling engine types (, , and) using detailed cfd modeling," *International Journal of Thermal Sciences*, vol. 132, pp. 411–423, 2018.

[40] M. J. Craun, "Modeling and control of an actuated stirling engine," Ph.D. dissertation, University of California Santa Barbara, 2015.

[41] Azelio. "Technology - building a renewable future." (2022), [Online]. Available: `https://www.azelio.com/the-solution/technology/`.

[42] D. Papurello, D. Bertino, and M. Santarelli, "Cfd performance analysis of a dish-stirling system for microgeneration," *Processes*, vol. 9, no. 7, p. 1142, 2021. DOI: `10.3390/pr9071142`.

[43] Qnergy. "Product - developer program." (2022), [Online]. Available: `https://qnergy.com/developer-program/`.

[44] B. Zohuri, *Heat Pipe Design and Technology*, Second. Springer International Publishing Switzerland, 2016.

[45] L. Krambeck, T. A. Alves, B. N. Felipe, M. d. A. Vinicius, and D. D. S. P. Henrique, "Thermal performance evaluation of different passive devices for electronics cooling," *Thermal Science*, vol. 23, pp. 1151–1160, 2 2019. DOI: 10.2298/TSCI170610300K.

[46] A. J. Clark, "Failures and implications of heat pipe systems," Sandia National Laboratories, Tech. Rep. SAND2019-11808, 2019.

[47] Y. Ma, E. Chen, H. Yu, *et al.*, "Heat pipe failure accident analysis in megawatt heat pipe cooled reactor," *Annal of Nuclear Energy*, vol. 149, no. 15 December 2020, 2020.

[48] T. K. Bera, "A magnetohydrodynamic (mhd) power generating system: A technical review," *IOP Conference Series: Materials Science and Engineering*, vol. 955, no. 012075, 2020.

[49] Electropedia. "Magnetohydrodynamic (mhd) power generation." (2005), [Online]. Available: https://www.mpoweruk.com/mhd_generator.htm.

[50] T. L. Benyo, "The effect of magnetohydrodynamic (mhd) energy bypass on specific thrust for a supersonic turbojet engine," NASA, Tech. Rep. NASA/TM-2010-216734, 2010.

[51] L. Vuskovic, S. Popovic, J. Drake, and R. Moses, "Magnetohydrodyanmic power generation in the laboratory simulated martian entry plasma," NASA Langley Research Center, Tech. Rep. 20050209960, 2005.

[52] J. L. Smith, "Magnetohydrodynamic power generation," NASA, Tech. Rep. NASA Technical Paper 2331, 1984.

[53] R. J. Litchford and N. Harada, "Multi-mw closed cycle mhd nuclear space power via nonequilibrium he/xe working plasma," in *Proceedings of Nuclear and Emerging Technologies for Space*, NASA Marshall Space Flight Center,

2011. [Online]. Available: https://ntrs.nasa.gov/api/citations/20110009914/downloads/20110009914.pdf.

[54] M. Tayal and M. Gacesa, "The essential candu," in W. J. Garland, Ed. UNENE, 2014, ch. Chapter 17: Fuel, pp. 1351–1422.

[55] V. Rohatgi, "High temperature materials for magnetohydrodynamic channels," *Bulletin of Materials Science*, vol. 6, no. 1, pp. 71–82, 1984. DOI: 10.1007/BF02744172.

[56] S. Anghaie, B. Smith, and T. Knight, "Direct energy converstion fission reactor," University of Florida, Tech. Rep. DE-FG03-99SF21894, 2022. [Online]. Available: https://www.osti.gov/servlets/purl/850575.

[57] C. N. R. C. (CNSC), "Rd-367 design of small reactor facilities," Canadian Nuclear Regulatory Commission, Tech. Rep. RD-367, 2011.

[58] Department of Energy - Office of Nuclear Energy. "What is a nuclear microreactor?" (Feb. 2021), [Online]. Available: https://www.energy.gov/ne/articles/what-nuclear-microreactor.

[59] J. Carlsson, "Inherent safety features and passive prevention approaches for pb/bi-cooled accelerator-driven systems," Stockholm, Sweden, Ph.D. dissertation, Royal Institute of Technology Department of Nuclear and Reactor Physics, Mar. 2003.

[60] M. Ruscak, T. Melichar, J. Syblik, *et al.*, "Energy well: Concept of 20 mw microreactor cooled by molten salts," *Nuclear Engineering and Radiation Science*, vol. 7, no. 2, 2021. DOI: 10.1115/1.4049715.

[61] I. A. E. Agency, *Advances in Small Modular Reactor Technology Developments*, 2020th ed. International Atomic Energy Agency. [Online]. Available: https://aris.iaea.org/Publications/SMR_Book_2020.pdf.

[62] Moltex Energy. "Technology suite." (2022), [Online]. Available: https://www.moltexenergy.com/technology-suite/.

[63] Energy Well. "Technical details." (2021), [Online]. Available: https://www.energywell.cz/technical-details#parameters.

[64] D. .-. O. of Nuclear Energy, "X-energy is developing a pebble bed reactor that they say can't melt down," US Department of Energy, Tech. Rep., 2021.

[65] P. Pappano, "Triso-x fuel fabrication facility overview," US Nuclear Regulatory Commission, commercial, 2018. [Online]. Available: https://www.nrc.gov/docs/ML1825/ML18254A086.pdf.

[66] C. F. Smith, W. G. Halsey, N. W. Brown, J. J. Sienicki, A. Moisseytsev, and D. C. Wade, "Sstar: The us lead-cooled fast reactor (lfr)," *Joural of Nuclear Materials*, vol. 376, no. 3, 2008. DOI: 10.1016/j.jnucmat.2008.02.049.

[67] J. Wallenius, S. Qvist, I. Mickus, S. Bortot, P. Szakalos, and J. Ejenstam, "Design of sealer, a very small lead-cooled reactor for commercial power production in off-grid applications," *Nuclear Engineering and Design*, vol. 338, pp. 23–33, 2018. DOI: 10.1016/j.nucengdes.2018.07.031.

[68] P. S. Fiske, "Preventing ice damage in potable water tanks," PAX Water Technologies, commercial, 2012. [Online]. Available: https://www.paxwater.com/hs-fs/hub/79614/file-15762477-pdf/docs/whitepaper_prevent_ice_damage_in_tanks.pdf.

[69] R. Moormann, "Phenomenology of graphite burning in air ingress accidents of htrs," *Science and Technology of Nuclear Installations*, vol. 2011, no. 589747, 2011. DOI: 10.1155/2011/589747.

[70] S. Stolyarov and A. Stolayrov, "Stirling generators: Challenges and opportunities," *Russian Electrical Engineering*, vol. 88, no. 12, pp. 778–782, 2017.

[71] D. Thimsen, "Stirling engine assessment," Electric Power Research Institute (EPRI), Tech. Rep. 1007317, 2002.

[72] A. Colmenar-Santos, D. Borge-Diez, and E. Rosales-Asensio, *District Heating and Cooling Networks in the European Union*. Springer, 2017. DOI: 10.1007/978-3-319-57952-8_1.

[73] A. Robinson, A. Eyres, S. Hudson, H. Hussain, and J. Young, "Ultra-high temperature thermal energy storage, transfer and conversion," in A. Data, Ed. Woodhead Publishing, 2020, ch. Chapter 9 - Dyanmic systems for ultrahigh temperature energy conversion, pp. 221–251.

[74] G. Marleau and R. Hebert A.; Roy, "Dragon release 3.06o," Ecole Polytechnique de Montreal, Tech. Rep., 2016.

[75] E. Varin, A. Hebert, R. Roy, and J. Koclas, "Donjon version 3.01," Ecole Polytechnique de Montreal, Tech. Rep., 2005.

[76] J. J. Duderstadt and L. J. Hamilton, *Nuclear Reactor Analysis*. Wiley Interscience, 1976.

[77] D. I. Poston, P. R. McClure, D. D. Dixon, M. A. Gibson, and L. S. Mason, "Experimental demonstration of a heat pipe - stirling engine nuclear reactor," *Nuclear Technology*, vol. 188, no. 3, pp. 229–237, 2014. DOI: 10.13182/NT13-71.

[78] F. Leszczynski, D. López Aldama, and A. Trkov, "Wims-d library update," International Atomic Energy Agency, Tech. Rep., 2007.

[79] A. Hebert, *Applied Reactor Physics*, third. Presses Internationales Polytechnique, 2020.

[80] M. Floyd, D. Leach, R. Moeller, R. Elder, R. Chenier, and D. O'Brien, "Behaviour of bruce ngs-a fuel irradiated to a burnup of 500 mwh/kgu," Atomic Energy of Canada Limited, Tech. Rep. AECL-10685, 1992.

[81] E. Nichita, "Retrofitting candu reactors for negative coolant void reactivity," *Transactions of the American Nuclear Society*, vol. 99, no. 717, pp. 777–780, 2008.

[82] M. Tayal and M. Gacesa, "The essential candu," in W. J. Garland, Ed. UNENE, 2014, ch. Chapter 18: Fuel Cycles, pp. 1423–1478.

[83] E. R. Masterson, *Nuclear Reactor Thermal Hydraulics - An Introduction to Nuclear Heat Transfer and Fluid Flow*. Taylor & Francis Group, LLC, 2020.

[84] P. M. Gerhart, A. L. Gerhart, and J. I. Hochstein, *Fundamentals of Fluid Mechanics*. Wiley & Sons, Inc., 2016.

[85] TerraPower. "Nuclear energy needs a domestic haleu supply chain." (2012), [Online]. Available: `https://www.terrapower.com/nuclear-energy-needs-a-domestic-haleu-supply-chain/`.

[86] Office of Nuclear Energy, Department of Energy, "Request for information (rfi) regarding planning for establishment of a program to support the availability of high-assay low-enriched uranium (haleu) for civilian domestic research, development, demonstration, and commercial use," *U.S. Federal Register*, vol. 86, no. 237, 2021.

[87] World Nuclear News. "Usa builds haleu supply chain." (2021), [Online]. Available: `https://www.world-nuclear-news.org/Articles/USA-builds-HALEU-supply-chain`.

[88] Z. He, Z. Liu, T. J. Marrow, and J. Song, "The infiltration behavior and chemical compatibility of molten lead-bismuth eutectic in nuclear graphite at elevated temperature," *Journal of Nuclear Materials*, vol. 550, no. 152921, 2021.

[89] H. Wang, J. Xiao, H. Wang, Y. Chen, X. Yin, and N. Guo, "Corrosion behavior and surface treatment of cladding materials used in high-temperature lead-bismuth eutectic alloy: A review," *Coatings*, vol. 11, no. 3, 2021.

[90] F. Garcia Ferre, A. Mairov, D. Iadicicco, *et al.*, "Corrosion and radiation resistance nanoceramic coatings for lead fast reactors," *Corrosion Science*, vol. 127, no. August 2017, pp. 80–92, 2017.

[91] K. Wasywich, "Characteristics of used candu fuel relevant to the canadian nuclear fuel waste management program," Atomic Energy of Canada Limited, Tech. Rep. AECL-10463, COG-91-340, 1993.